Long-term morphodynamic behaviour of the Maasvlakte 2 sand extraction pits and the influence on surrounding sand wave fields.

MSc Thesis in Civil Engineering and Management
Britt de Groen
march, 2014

UNIVERSITY OF TWENTE.

Royal Netherlands Navy

Rijkswaterstaat
Ministerie van Verkeer en Waterstaat

Long-term morphodynamic behaviour of the Maasvlakte 2 sand extraction pits and the influence on surrounding sand wave fields.

MSc thesis in Civil Engineering and Management
Faculty of Engineering Technology
University of Twente

Student:	Britt de Groen BSc.
Location and date:	Enschede, March 26, 2015
Thesis defense date:	April 2, 2015
Graduation supervisor:	Prof. dr. S.J.M.H. Hulscher (University of Twente)
Daily supervisor:	Dr. ir. B.W. Borsje (University of Twente)
	Dr. ir. P.C. Roos (University of Twente)
External Supervisors:	Ir. T. Ligteringen (Royal Netherlands Navy)
	Drs. A. Stolk (Ministry of Transport, Public Works and Water Management)

Voorwoord

Hier voor u ligt de afstudeerscriptie, waar ik het laatste half jaar aan gewerkt heb. Met het beëindigen van dit project rond ik ook het laatste deel van mijn studie af. Het project over de zandwinputten van de tweede Maasvlakte heb ik met plezier gedaan. Zowel het technisch als het praktische aspect kwamen er beide in voor. Dit zorgde voor afwisseling in de opdracht en heeft er toe geleidt dat ik veel verschillende mensen heb ontmoet.
Ik wil Leendert en Ad bedanken voor de mogelijkheid die ze mij gegeven hebben om het onderzoek uit te voeren, maar vooral voor de kritische houding en de focus op het praktische gedeelte. Daarnaast wil ik Suzanne bedanken voor de feedback gesprekken en dat ik mee mocht naar de leerzame en gezellige NCK dagen!
Bas, bedankt voor je enthousiasme, je relativeringsvermogen en je Matlab-skills. Je hebt me enorm geholpen met aandachtig te kijken naar data, niet te stressen en vaak heb je me een glimlach bezorgd. Bedankt!
Pieter, jou wil ik bedanken voor je geduld en de hulp met het model. Je feedback was altijd duidelijk en kon altijd bij je binnen lopen, dat was heel fijn.
Thijs, je hebt me eeen kijkje gegeven in de wereld van de Marine, wat voor mij geheel onbekend was. Bedankt voor de leuke en leerzame gesprekken, je hebt ervoor gezorgd dat ik me de dagen in Den Haag erg op me gemak voelde!
Daarnaast wil ik de Dienst der Hydrografie bedanken voor de leuke gesprekken en vaste lunchpauzes, het waren fijne weken! Daniëlle bedankt voor de wondere wereld van de bathymetrie, je enthousiasme en hulp, waar ik maar vragen kon! Martien bedankt voor je kritische kijk op mijn scriptie en de gezellige koffie momenten! John, bedankt voor een onvergetelijk weekend op de Luymes, het was geweldig!
De studenten in de afstudeerkamer wil ik graag bedanken voor het accepteren van een chaotisch bureau en daarnaast voor de oneindige wandelingen richting het koffiezetapparaat.
Lieve vrienden, bedankt voor de fantastische jaren die ik in Enschede heb mogen meemaken. Bedankt voor de vriendschap, gezellige avonden en gesprekken, zonder jullie was het een saaie boel geweest!
Lieve Leonie, bedankt voor een fijne thuishaven en dat je altijd voor me klaar staat, vooral tijdens de laatste loodjes.
Tot slot wil mijn lieve ouders bedanken, voor de mogelijkheid die ze mij gegeven hebben om te studeren en mezelf te ontwikkelen. Ik kan jullie niet beschrijven hoe erg ik dat waardeer en hoeveel liefde jullie mij geven.
Last but not least, wil ik Tycho bedanken, voor je positiviteit, hele fijne weekenden en je geduld. Je bent de liefste en nu is het tijd voor onze toekomst samen, ik ben er klaar voor!

Liefs, Britt Maart, 2014

Abstract

The Rotterdam harbour is one of the largest harbours in the world and still expanding. The most recent expansion is called Maasvlakte 2 (MV2), which added 2000 hectares to the west of the existing port into the sea. MV2 was realised between 2009 and 2013 using sand dredged some kilometres offshore in the North Sea. A total of 200 million m3 sand was extracted from two sandpits with volumes of 170 Mm3 and 30 Mm3 . Those sandpits are located nearby the navigation channel to Rotterdam and surrounded by sand wave fields. Since sand waves have a migration rate in the order of 5 meters per year and a height of 5 meters, they can hinder navigation. Therefore it is important to know how sand wave fields behave. The purpose of this study is to determine the long-term effects of the sandpits of Maasvlakte 2 on the surrounding sand wave fields.

This is study is done by a data analysis of bathymetric data and secondly a model study for the long-term behaviour of sand pit and the sand wave fields. The bathymetric data is gathered from the anchorage area, a sand wave field 6 km away of the sand pits. These bathymetric data is analysed by a Fourier analysis (van Dijk et al. 2006) to calculate the specific sand wave characteristics. With a linear regression method the migration rate is determined for the sand waves. This is done for the period between 2006 and 2014, divided into two stages, one before and one after the realisation of the sandpits.

The sand waves show a dynamic migration rate, with a range between 4.0-5.8 m/year. Before the realisation of the sandpit the range was between 3.9- 6.9 m/year and in the after stage a range of 2.6- 5.8 m/year. Because the calculation of these migration rates is very dependable of the place and angle, there cannot be made a conclusion based on this results.

Modelling the long-term behaviour is done in two steps: (i) by modelling the sandpit in an idealized morphodynamic model (Roos et al. 2008) and, (ii) to use these results as input for a smaller-scale idealized sand wave model (Besio et al. 2006). The sandpit model is forced by tidal flow conditions as they apply near the sandpits, and the sandpit geometry is taken from recent surveys.

Next, a simulation is carried out indicating how the pit will deform and migrate over the next century. Throughout this evolution, and at fixed locations, the tidal flow pattern and local depth can be extracted. This flow pattern and local depth are used as local forcing for the smaller-scale

sand wave model.

The sand wave model in the second step uses linear stability analysis to estimate the sand wave characteristics such as wavelength, orientation, growth and migration rates. Being driven by the gradually changing flow conditions and depth from the sandpit model, it indicates how the sand wave characteristics are affected by pit evolution.

The models show the following long-term behaviour of the sandpits: The edges will flatten out, the little pit will move to the larger sandpit and the pits will move with the dominant flow direction. When the navigation channel is also implemented into the model, the ridge between the pits and the channel will gradually vanish. This eventually results in one large pit. The dredging activities of the channel are not taken into account in the model.

When looking again to the situation without the navigation channel, all sand wave fields surrounding the pits have crests with a north-east orientation. Those sand wave fields have the same response time as the Westhinder sand wave field, in the Belgium sea shelf. At the centre of the pit, sand waves will appear as well which have also crests with a north-east orientation. However, this orientation fluctuates with a small range throughout the years. If in reality there is silt present at the centre of the pit, which is most likely, no sand waves will arise.

It can be concluded that the sandpits do not have a large impact on their surroundings. This is positive for the navigation maintenance, because no large changes will be expected over time.

Contents

Chapter 1

Introduction

The landscape of the seabed changes by sedimentation and erosion, this is due to a storm or tidal currents. Because of the large changes it is important to study the marine-morphodynamics, especially for the seabed. This study concentrates on the morphodynamic behaviour in the North Sea.

The North Sea is situated between The Netherlands, Germany, Denmark, Norway, United Kingdom, France and Belgium (see Figure 1.1). A very busy shipping route is located in the southern part of this sea, which connects Northwest Europe to the rest of the world. Besides shipping, fishery, cables, pipelines, wind farms, gas-, sand- and oil extraction are important activities taking place in the North Sea.

An important harbour in the North Sea is the mainport of Rotterdam. To enable economic growth an extension was needed. Therefore the second Maasvlakte was built as enlargement of the mainport. For this enlargement approximately 200Mm^3 sand was needed. This sand was extracted from the bed of the North Sea.

Figure 1.1: Location of the North Sea (source: home.comcast.net, 2014)

The amount of sand is dredged between 2008 and 2013 (Havenbedrijf Rotterdam, 2009). Mostly the maximum dredge depth is two metres, for this project an exception is made by Rijkswaterstaat (Dijkshoorn and Stolk, 2009). Two sandpits arose with larger depths; a large sandpit with an area of 13.2 km^2, a depth between 10-20 metres below the original sea bed and a volume of 170Mm^3 and a smaller sandpit with a volume of 30Mm^3, an area of 2.6 km^2 and a depth between 10-12 metres below the original sea bed (Dijkshoorn and Stolk, 2009; Schipper, 2014).

There was not a lot experience with that amount of dredged sand, only with smaller amounts. For instance between 1996-2000, there were two pits created; the 'Drawing Pin' pits and the PUTMOR pit. The 'Drawing Pin' pits were temporary sand extractions in the near shore coastal zone and were relatively deep - up to a maximum of 20 metres below the local sea bed elevation - with steep slopes. The 'Drawing Pin' pits were located by Heemskerk/Wijk aan Zee (Hoogewoning and Boers, 2005). There was sedimentation in the pit and the slopes were slightly levelling of (Hoogewoning and Boers, 2001). The PUTMOR pit was a large-scale- and deep-extraction pit outside the coastal zone, located in the north of the Euro-Maas channel (Hoek van Holland) and research was executed to obtain more knowledge on sandpits with an extraction depth deeper than 2 metres. This sandpit had a volume of 4.5Mm^3, with a surface area of 0.65 km^2 and a depth varying between 5 and 12 metres (Boers, 2005). Svašek (2001a,b,c) conclude with a field study that the influence of the sandpit on the flow velocities is generally small and that there was no morphological evolution visible in the measuring period.

Figure 1.2 shows the location of the two sandpits used to realise Maasvlakte 2 and the channel of Rotterdam mainport. The main waterway to enter Rotterdam mainport is the Eurogeul channel (2) which passes into the Maasgeul channel (1). Between the two channels is an area to turn the vessels, the turning basin (3). At the beginning of the Eurogeul channel is an anchorage area for vessels to wait before entering Rotterdam mainport.

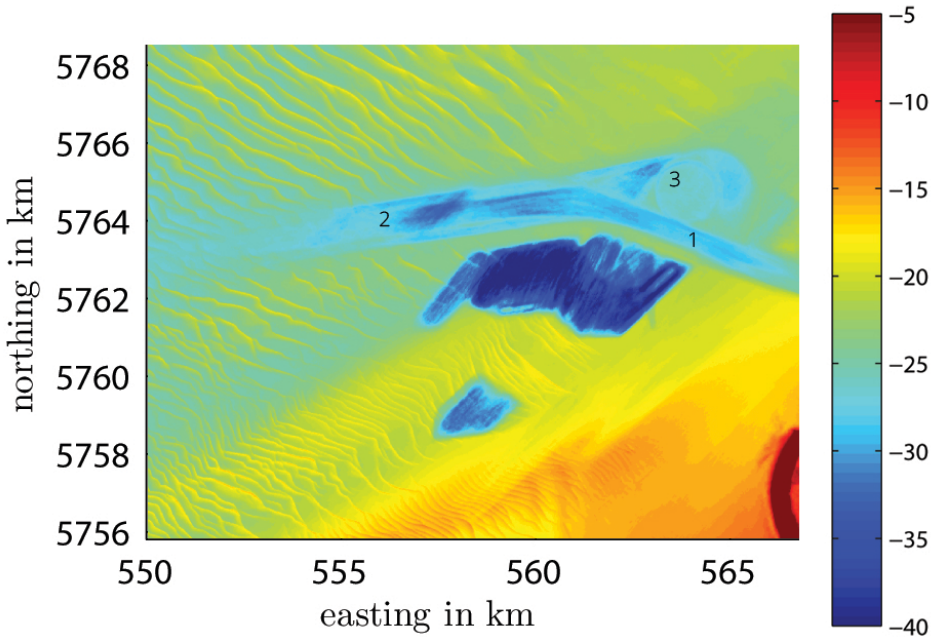

Figure 1.2: Location of the sandpits and channels and the depth in meters. (2.Eurochannel, 1.Maaschannel, 3.turn-channel) [source: HNLMS Snellius, 2012]

In Figure 1.2 the different seabed patterns are also visible. For instance at the south-west side of the pits the sand waves have typically wave lengths of 500 metres and a height of 5 metres (Dorst, 2009). When sand waves are clustered, they are defined as sand wave fields. Depending on the flow conditions, sand waves could migrate up to 10 metres per year. The migration takes also place into the navigation channels, this could cause a reduction of the depths, which has negative effects on the entrance of the mainport. Besides the effects on the navigation channels also pipelines and cables could be damaged and exposed. Rijkswaterstaat (Department of Waterways and Public Works in The Netherlands) is responsible for a guaranteed of depth in the navigation channels. They realise this by dredging the navigation channels, turning basin and anchorage areas. Without the maintenance of the channels, Rotterdam is not accessible for vessels with a deep draught (>22.55m), which is negative for the activity of the mainport.

1.1. Problem definition

The behaviour of the sandpit in coastal environment strongly depends on the sediment supply, hydraulic conditions and orientation of the pit (Van Rijn and Walstra, 2004). Following Roos et al. (2008) a modelled sandpit with a volume of 48Mm^3 and a depth of 2 metres has an impact on the morphological dynamics of the surroundings. The size of the impact depends on time, bottom friction, Coriolis and orientation of the pit with respect to the tidal flow. The realised sandpits from Maasvlakte 2 have a much larger depth, namely between 10 and 20 metres. According to Klein and van den Boomgaard (2013), who studied the evaluation of the two sandpits with a hydraulic model, the sandpit will silt up and sharp edges will flatten over the years. These studies are based on hydrodynamic and morphological models. After the creation of the sandpits there are a lot of changes in the North Sea. These changes will cause dynamic changes in the surrounding area of the sand pit (for example: wave height, flow velocity etc.), where sand waves fields are situated. The normal sand wave migration rate in this area is 10 metres per year (Dorst, 2009), while the data study from Schipper (2014) shows a more dynamic migration rate.

For the navigation in the North Sea it is important to predict the behaviour of the sand wave fields. Because the ships have to take into account the place and height of the sand waves. The current problem is that there is no experience with large dimensions of a sand extraction pit, especially with a large depth. This has consequences on the morphodynamic behaviour, which influence the surroundings, where sand waves are present.

1.2. Research objective

The objective of this thesis is to understand the morphodynamic behaviour of the sandpit and the influences of the surrounding sand wave fields.

Based on this objective, the following research questions are addressed:
- Which morphological behaviour in- and outside the sandpits is visible over 200 years?
- Are there sand waves arising inside the pit?
- What is the influence of the sandpit on the surrounding sand wave fields and are these influences also visible in the bathymetric datasets?

1.3. Methodology

To study the research objectives, a methodology is used with several models. Because there is not a model which is capable to model the extracted sandpit and the occurrence of sand waves, the modelling approach is done in two steps.

To implement the sandpits an idealised morphodynamic model is used from Roos et al. (2008). This model has a little calculation time and is forced by tidal flow conditions near the sandpits. The simulation is carried out indicating how the pit will deform and migrate over time. At fixed locations the tidal flow patterns and depth can be extracted.

The model of Besio et al. (2006) is used to study the occurrence of the sand waves. This is a smaller-scale idealised model, with a linear stability to estimates the sand wave characteristics as wave length, orientation and growth rates. Also this model has a little calculation time and is forced by tidal flow conditions, grain size and water depth.

In order to achieve the research objective and to answer the research questions, the following methodology is used:

- Gathering bathymetric data to implemented the realised pits into the sandpit model. This is done by the Hydrographic Service of The Netherlands Navy, they gather data from hydrographic survey vessels and make nautical charts of these bathymetric data.
- Analyse the quality of the bathymetric datasets in surrounding sand wave fields of the extracted sandpits. This is done by method of Van Dijk et al. (2008) which calculates the position and wave length of the sand waves. Finally with the calculated sand wave characteristics the migration is calculated.
- Next, the bathymetric data and the tidal flow conditions need to be transformed into an input for the sandpit model of Roos et al. (2008). After the transformation the model can be ran with the specific conditions for this case.
- With the output of the sandpit model the morphodynamic behaviour of the sandpits are visible. The model simulates the deform and migration of the sandpits by calculating the local depth. This is done for the situation with- and without the extracting sandpits for the period 0 to 200 years.
- The local depth and flow conditions are calculated for fixed locations. Namely, the deepest depth in the pit, in the anchorage area, in a non-influenced area and at existing sand wave fields. This output can be used as input for the sand wave model of Besio et al. (2006). This model calculates if the circumstances are present for sand wave occurrence. When sand waves occur, the model calculates the characteristics as wave length and growth rate. With this information a conclusion can be made by the evolution of sand wave fields and if the characteristics are influenced by the realisation of the sandpit.
- Finally, the modelled data is compared with the available bathymetric data and can be concluded if the same evolutions are visible.

1.4. Reading guide

Chapter 2 – Case description: a description of the Maasvlakte 2 and the basics of sand waves and sandpits.
Chapter 3 – Bathymetric data study: how are bathymetric surveys performed, the method of analysing the available data on specific locations and the calculations of the migration rate of sand waves.
Chapter 4 – Model description: description of the model from Roos et al. (2008) and Besio et al. (2006) and the used input and output of the models.
Chapter 5 – Results: the results of the morphological behaviour of the sandpits, the sand wave characteristics at different locations, the interaction between the sandpits and navigation channel and answers to the first and second research questions.
Chapter 6 – Discussion: discussions of the input of the models and the availability of bathymetric data.
Chapter 7 – Conclusions: the final conclusions and answers to all research questions.
Chapter 8 – Recommendations: the recommendations for further researches.

Chapter 2

Background information

The North Sea is a dynamic area where many processes take place. In this chapter relevant background information is given about the second Maasvlakte and sandpits as well as extra information about sand waves.

2.1. Maasvlakte 2

The Rotterdam harbour is one of the biggest harbours of the world and the biggest harbour in Europe (JOC, 2012). In 2004 the harbour of Rotterdam was beaten by Shanghai, to stay at a high position extension was needed (AAPA, 2004). The expanded harbour increased the economic value of the harbour, for now and in the future. The expansion of the Rotterdam harbour is called the Maasvlakte 2 and Figure 2.1 gives a representation of the present situation. Maasvlakte 2 is a location for port activities and industry, immediately to the west of the present port and industrial area. Maasvlakte 2 adds 2000 hectares to the existing port into the sea, the dredging activities were performed between 2009 and 2013 (Dijkshoorn and Stolk, 2009). It is conceivable that this extension is very radical for the surroundings both onshore and offshore. The extension is made by sand dredged from the North Sea, about 11 km near shore (Port of Rotterdam, 2014).

Figure 2.1: Maasvlakte 2, in orange the extension with respect to the 'first' Maasvlakte.(source: Havenbedrijf Rotterdam N.V., Projectorganisatie Maasvlakte 2.)

2.2. Sandpit

From research of Klein (1999), Hoogewoning and Boers (2001), Van Rijn and Walstra (2002), Roos et al. (2008), Roos et al. (2004), it has been found that both the orientation of the sandpit with respect to the dominant flow direction and the dimensions of the sandpit have an influence on the hydro- and morphodynamic response of the pit. Following De Groot (2005) there are some aspects which determine the local flow pattern, namely:

- Dimensions of the sandpit
- Angle between the main pit axis and direction of approaching current
- Strength of the local current
- The bathymetry of the surrounding area

The orientation of the sandpit with respect to the direction of the local current is important for the flow velocity inside and outside the pit. When the local current is situated perpendicular to the major axis of the sandpit, the velocities in the deeper zone are reduced due to the increased water depth. The orientation of the sandpit with respect to the current can also be parallel. The flow velocities in the pit will increase due to the decrease of bottom friction. Just upstream of the pit, flow contraction will occur which results in a local increase and decrease of the flow velocity (Van Rijn and Walstra, 2004). The main axis can also be oblique to the flow, in that case both effects will appear (perpendicular and parallel). This will lead to flow refraction. Following De Boer et al. (2011), a large sandpit construction of the coast of The Netherlands will significantly influence the tidal flow up to hundreds of kilometres away.

Following Hoogewoning and Boers (2001), the morphological effect of a sandpit, situated perpendicular to the dominant tidal current direction, expected comparable to the present navigation channel:

- ▷ The greatest changes in the bed elevation occur around the in and out flow of the pit.
- ▷ The slopes of the pit will decrease.
- ▷ Sedimentation will settle in the centre of the pit.
- ▷ The centre of the pit will shift in the direction of the flow.

2.3. Sand waves

The sandy sea floor is covered by a variety of rhythmic features. All the bed forms have their own characteristics. In Table 2.1 the most important bed forms are listed with their typical wavelength, amplitude and migration rate.

	wavelength	**max. height**	**migration rate**
ripples	∼1 m	0.01 m	∼1 m/hour
mega ripples	∼10 m	0.1 m	∼1 m/day
sand waves	∼500 m	5 m	∼10 m/year
sand banks	∼6 km	10 m	∼1 m/year

Table 2.1: Characteristics of rhythmic features of the seabed (Dorst, 2009).

The wave length is the distance between two minimal trough depths of the sand waves. Furthermore, a sand wave has a stoss- and a lee side, a crest- and a trough part. These terms are illustrated in Figure 2.2. The tidal sand waves are important for this research and therefore explained more in the following paragraphs. First occurrence is discussed, followed by the explanation of the sand wave theory and finally the migration.

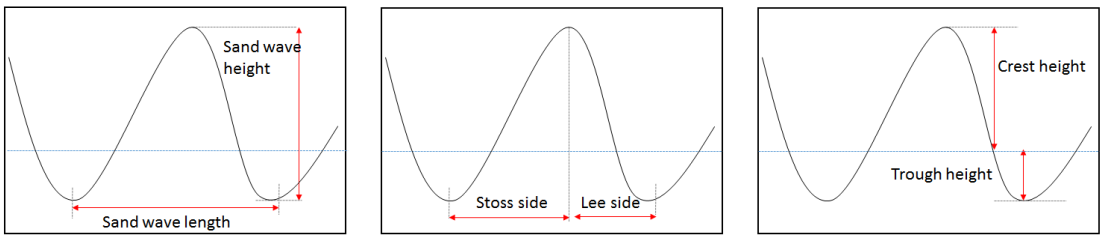

Figure 2.2: Terms of sand wave characteristics.

2.3.1. Occurrence

In the North Sea many sand waves are present. The sand waves are mostly clustered and these clustering's are called sand wave fields. The crests are often assumed to be perpendicular to the principal current Johnson et al. (2009); Langhorne (1981); Tobias (1988). Based on a theoretical analysis, Hulscher (1996) arrived at the conclusion that sand wave crests may deviate up to 10◦ anti-clockwise form the direction perpendicular to the principal current. Figure 2.3 shows the location of sand banks and the sand wave fields in the North Sea.

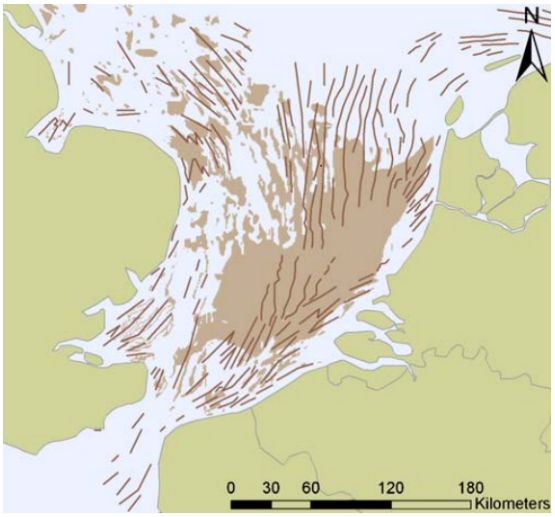

Figure 2.3: Sand banks (lines) and sand wave fields (brown area) (Van der Veen et al., 2006)

2.3.2. Sand wave theory

Sand waves are formed because of positive feedbacks between tidal currents and a sandy bed. Since a bed is never completely flat, these oscillating currents result in vertical recirculating cells, which transport sediment from the troughs to the crests.

Due to the interaction with the tidal currents free instabilities in a morphodynamic system can lead to growing bed forms (Huthnance, 1982). On the bed there are little perturbations, the flow velocity driven by the tidal currents is disturbed by this perturbations. The flow velocity is accelerating upstream, the disturbance and decelerating downstream (see Figure 2.4a). When the flow passes through a tidal cycle, ebb and flood, the velocity pattern of Figure 2.4a happens in opposite direction, this is shown in Figure 2.4b. When this pattern is averaged over a tidal cycle it turns out that there is a velocity towards the crest at the bottom and a velocity in the opposite direction in the water column. This results in vertical circulating cells (Hulscher, 1996) and shown in Figure 2.4c. The flow near the bed towards the crest makes the disturbance to grow. The growing of the disturbance is beside the flow also dependable of the sediment transport. When the bed shear stress exceeds a critical value, sediment is able to transport. The bed shear stress is determined by the sediment grain size, roughness and the flow velocity. There are

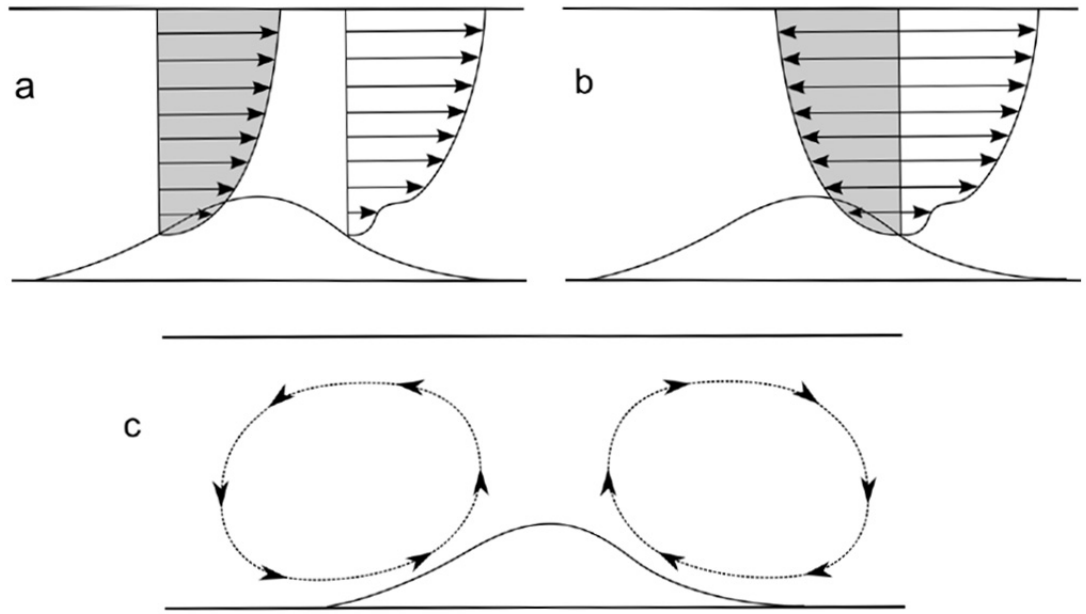

Figure 2.4: Flow field upstream and downstream of a sand wave for flow in one direction (a), flow field on one side of a sand wave for flow in ebb and flood directions (b) and vertical recirculating cells (exaggerated) as a result of a tide averaged flow on both sides of a sand wave (c) (Choy, 2015)

two types of sediment transport; bed load and suspended load transport. Bed load transport is in contact with the bed and occurs by larger grain sizes or small shear stresses, while suspended load float in the water column and occurs by smaller grain sizes or larger shear stresses. Therefore there are some conditions for the occurrence of sand waves namely, a current with a velocity of 0.4-1 metre per second (Hulscher, 1996; Knaapen and Hulscher, 2002; Tonnon et al., 2007) and a grain size of the sediment with a medium grain size range of 0.2 to 0.5 mm (Tonnon et al., 2007). With the bed load transport the sediment can roll or jump. Commonly, this transport only occurs in a thin layer above the bed (Thorn, 1987). Borsje et al. (2013) showed with a numerical morphodynamic model that suspended load have a damping effect on sand waves, while bed load transport have a growing effect. Finally, when sand waves grow too high, their slopes may get too steep for grains to be transported uphill and, consequently, sediments will be transported downhill more easily because of gravitational effects. In modelling sand waves these processes are covered by the slope effect. So the slope effect will also suppress sand wave growth (Borsje et al., 2013).

2.3.3. Migration

Following Besio et al. (2004) and Nemeth et al. (2002) they considered horizontal migration of sand waves due to asymmetries in the tidal flow. In Figure the circulations cells and the bed forms show stable pattern, when there is a disturbance in the tidal flow this results in an asymmetric profile of them both. The residual flow is responsible for the disturbance in the tidal flow, which result in sand wave migration, in the direction of the residual current.

The migration of the sand waves is very important in respect to the navigation channels. As can be seen in Figure 2.3 the sand waves are located near the navigation channels. When the sand waves migrate into the navigation channels, it is possible the channels are not deep enough to let ships pass. Rijkswaterstaat is responsible for the maintenance of the channels and has to guarantee a minimal depth. This is done by dredging the navigation channel throughout the year. A lot of pipe and cable lines lie in the seabed, like electricity, telephone, oil and gas lines. The diameter of the pipelines are between the 0.1 and 1.5 metres and are buried minimal 0.2 to maximal 2 metres in the seabed (Morelissen et al., 2003). Because there is migration of the sand waves and other bottom patterns, the cables and pipes can be exposed (Figure 2.5).

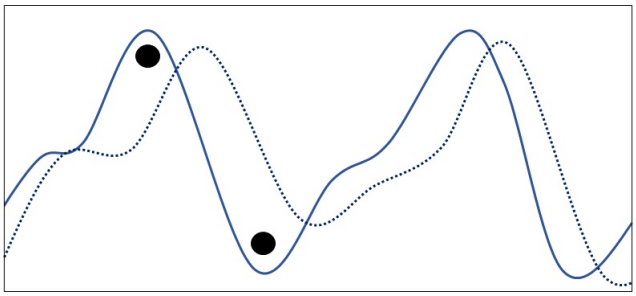

Figure 2.5: Exposing of pipelines, the solid line represent the original sand wave and the dashed the migrated sand wave. The black circles are the pipelines.

Chapter 3

Bathymetric data study

The first part of this study is to analyse bathymetric data. For the collection of bathymetric data vessels are used to survey the sea bed. The influence of the sandpits on current sand wave fields is analysed in this bathymetric data study. This chapter describes the analysis from the bathymetric data collection to results. First the studied location has to be determined and after that the bathymetric data is implemented in the method of Van Dijk et al. (2008) to get the sand wave characteristics. Following up, the migration rate of the sand wave fields are determined by linear regression.

3.1. Collecting bathymetric data

The Hydrographic Service of the Royal Netherlands Navy is the government office which informs mariners about shipping channels, the seabed and underwater hazards such as obstructions like wrecks. In order to be able to inform them, the Hydrographic Service produces nautical charts and products, and issues Notices to Mariners. The nautical charts are based on bathymetric surveys which are done with two vessels of the Royal Netherlands Navy; HNLMS Luymes and HNLMS Snellius. Because the sea floor is changing with time, the bathymetric surveys should be carried out regularly. To survey the sea floor the vessels have to carry a lot of equipment. In the next paragraph 3.1.1, the sensors on the vessels will be explained.

3.1.1. Collecting devices

The measuring equipments have to collaborate with each other to give a view on the sea floor. Figure 3.1 gives an overview of the different devices and explained briefly.

Singlebeam echo sounder: The singlebeam echo sounder measures the water depth directly beneath the vessel. The hull-mounted transceiver transmits a high-frequency acoustic pulse in a beam directly downward into the water column. Acoustic energy is reflected off the sea floor beneath the vessel and received at the transceiver. The transceiver contains a transmitter, which controls pulse length and provides electrical power at a given frequency. To calculate the actual speed of sound through the water column the salinity, temperature and pressure need to be taken into account. This transmit-receive cycle repeats at a fast rate, in the order of milliseconds. On board the vessels, three single beams are present, each has its own frequency to detect different types of soil. The single beam is nowadays used as a control device for the multibeam echo sounder.

Multibeam echo sounder: A multibeam echo sounder is a device to determine the depth of water and nature of the seabed. The multibeam transmits acoustic waves in a shape of a fan from directly beneath the vessel's hull. The system measures and record the time it takes for the acoustic signal to travel from the transducer (transmitter) to the sea floor and back to the receiver. In this way, the multibeam transducer produces a "swath" of soundings for broad coverage of a survey area. The coverage of the sea floor depends on the depth of the water, typically two to four times the water depth.

Side Scan Sonar (SSS): The SSS emits pulses down toward the seafloor across a wide angle perpendicular to the path of the sensor through the water. The intensity of the acoustic reflections from the sea floor is recorded in a series of cross-track slices. These slices form an image of the sea bottom with the coverage width of the beam. It looks like a movie and is used to provide the difference in texture of the sea bottom and to discover pipelines, wrecks and obstruction at the bottom. The SSS is towed around 100 metres behind the vessel.

Magnetometer: The magnetometer is used to detect metal objects at the sea bottom, such as pipelines, cables and part of wrecks. The magnetometer is towed approximately 250 metres behind the vessel, if this distance becomes less, the magnetometer will detect the vessel itself.

Moving Vessel Profiler: The Moving Vessel Profiler (MVP) is dropped into the water every 15 minutes and will measure the speed of sound at various depths through the water column. The probe will measure temperature, speed of sound and pressure. The sound velocity through the water column will change, caused by changing temperatures, pressure and salinity of the water. The speeds of sound will be applied to the multibeam and singlebeam echo sounders to establish the correct depth values.

Global Navigation Satellite System (GNSS): GNSS is a satellite navigation system with global coverage. Two GNSS systems are GPS (Global Positioning System) and GLONASS (Global'naya Navigatsionnaya Sputnikovaya Sistema). Without using a positioning system on board the surveys are not accurate.

Motion Reference Unit (MRU): The MRU is a heave, roll and pitch sensor to compensate for the vertical and horizontal movements of the echo sounder's transducer and positioning system's antenna.

The systems on board of the vessels are much more complicated and extensive, which is not relevant in this research.

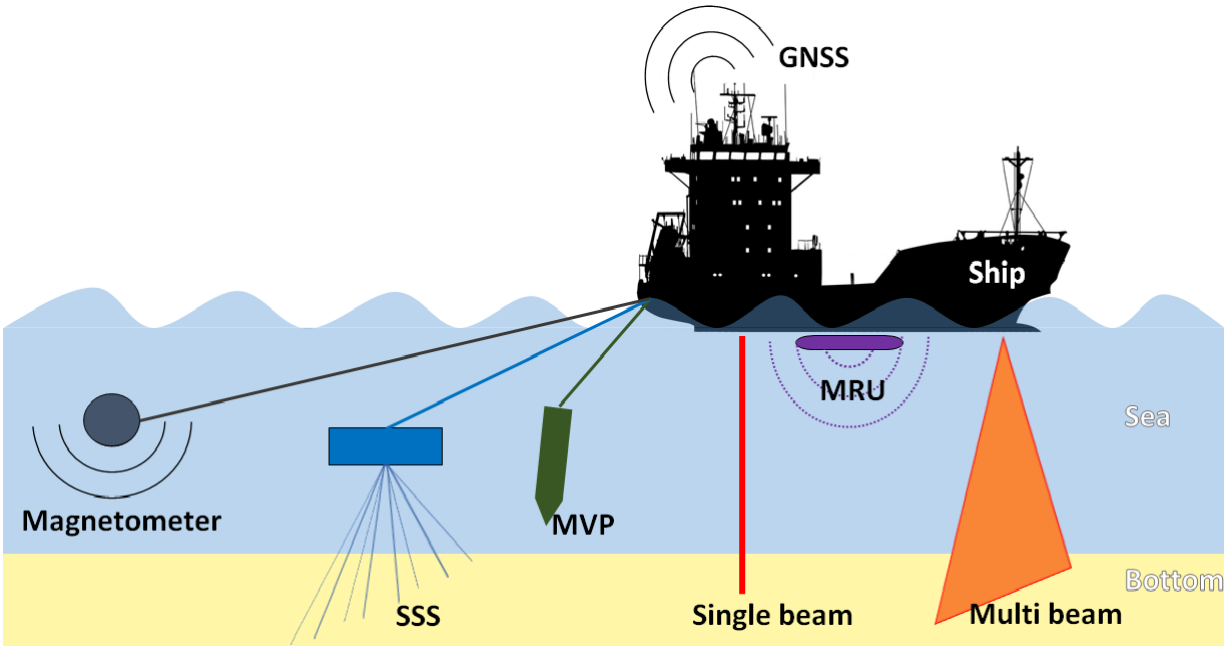

Figure 3.1: Several devices at a Marine ship of the Hydrographic Service

3.2. Location of the bathymetric data study

The requirements of selecting data are:

- The surrounding of the sandpit
- Data has to be available over more years
- The quality of the data has to be sufficient

The location of the data is based on the research by Svasek Hydraulics (Klein and van den Boomgaard, 2013). Svasek has, on behalf of Rijkswaterstaat, modelled the consequences of the realisation of the pits based on hydrodynamic effects. The data location is chosen based on the results of Svasek of the most effective area due to flow direction and velocity. First the flow velocity was depth averaged, but they recalculated those values with the assumption of logarithmic velocity profile to the velocity at the water surface (Klein and van den Boomgaard, 2013). Figure 3.2 illustrates the change in velocity at the water surface and flow direction for low and high tides.

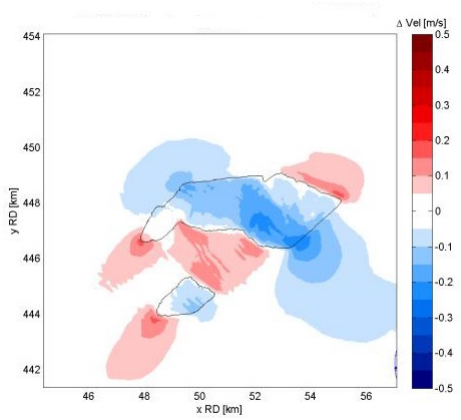

(a) Maximal change in velocity by low tide including wind with respect to an undisturbed bottom

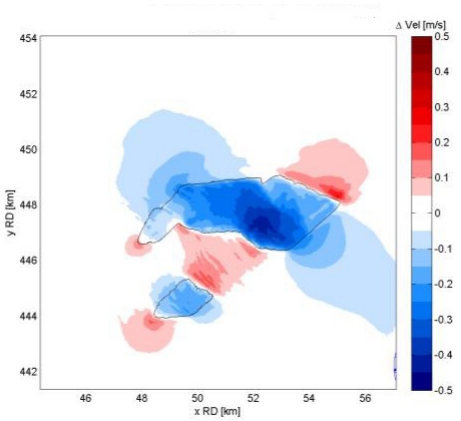

(b) Maximal change in velocity by high tide including wind with respect to an undisturbed bottom

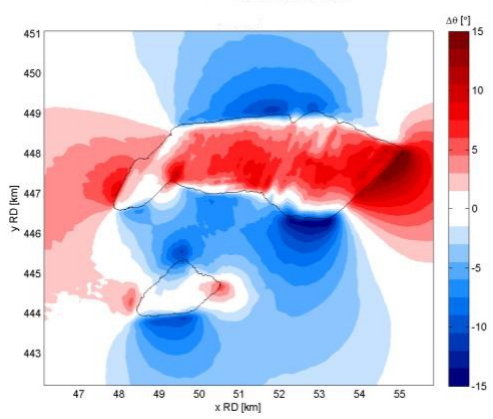

(c) Absolute difference in flow direction by low tide including wind

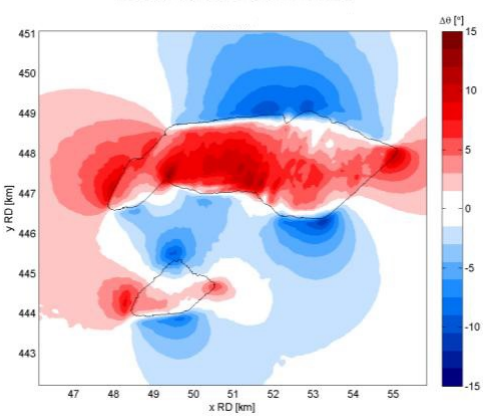

(d) Absolute difference in flow direction by high tide including wind

Figure 3.2: Maximal changes and influence of the pits (Klein and van den Boomgaard, 2013)

The area southwest of both of the pits is the most influenced area (as seen in Figure 3.2). The bathymetric survey has to be surveyed with a multibeam echo sounder, because this survey has more data than singlebeam survey. Because the multibeam has been introduced from 2004, only from that moment the data is taken into account. The available bathymetric survey is illustrated in Figure 3.3. Three areas are selected; the green areas A, B and anchorage area. In first instance the two upper areas were ideal, because in- and outside the influence area the data can be analysed. Unfortunately the quality did not fulfil the requirements.

Table 3.1 gives a summary about the bathymetric surveys of the three areas. Area A and B are based on three data sets, one set from 2004, which was the first official survey with the multibeam echo sounder. This set gave an impression of the sea bottom geometry, but a lot of adjustments were made, which makes it unsuitable for analysis. The data from 2008 is doubtful, not all the data was gathered by the Hydrographic vessels and a lot of unknown adjustments were made by another company. These surveys are also not suitable for data analysis. The survey time is 2 years, which is very long for such a dynamic area. For area A and B the only data which remains for analysis is from 2012, which is not enough. The 2008 dataset from the anchorage area is surveyed and adjusted by Rijkswaterstaat, this data is the most trustful data from the 2008 series. The described reasons conclude that only the anchorage area is taken into account. A disadvantage of the anchorage area is that it is not located in the influenced area following Klein and van den Boomgaard (2013), so the influences of the pits are less visible in the analysis.

Table 3.1: The bathymetric surveys of the area around the sandpit. The HY stands for a survey of the Hydrographic Service and the first two numbers are representing the year.

Area A	Area B	Anchor Area	Notes
HY04156-157	HY04156-157		First multi beam survey
HY08111-9	HY08111-8	HY08111-1	9 and 8 unusable, 1 usable
HY12111	HY12111		Usable
		HY11324-12105	Usable
		587-13	Usable (RWS)
		HY14105	Usable

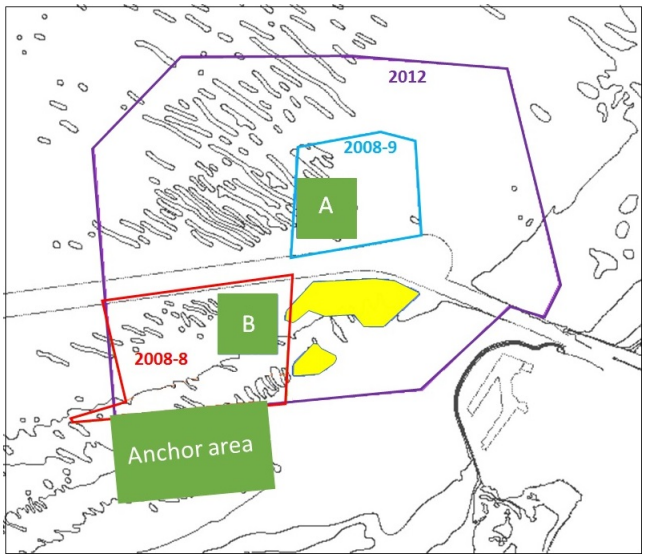

Figure 3.3: Location of the data sets and the surveys

3.3. Bathymetric data analysing

The data analysis consists of three parts: first gathering the data, secondly determine the wave length and crest- and trough positions and at last calculate the migration rate. In the next paragraphs the methods will be described briefly, not with a lot of details.

3.3.1. Method description to analyse the data

The data is gathered from the Hydrographic Service from the data sets as described in Section 3.2. The transect is located in the middle of the sand wave field and as much as possible selected perpendicular to the sand wave crests. The bathymetric data sets are all gathered at the same transect position in the anchorage area, which is represented with a black line in Figure 3.4. The height data is collected along the transect. A 1-D Fourier analysis is applied to the data, to separate sand waves from other bed forms by discarding wavelengths that do not correspond to the sand wave length spectrum. Following (Van Dijk et al., 2008) this sand wave length spectrum has to be chosen carefully.

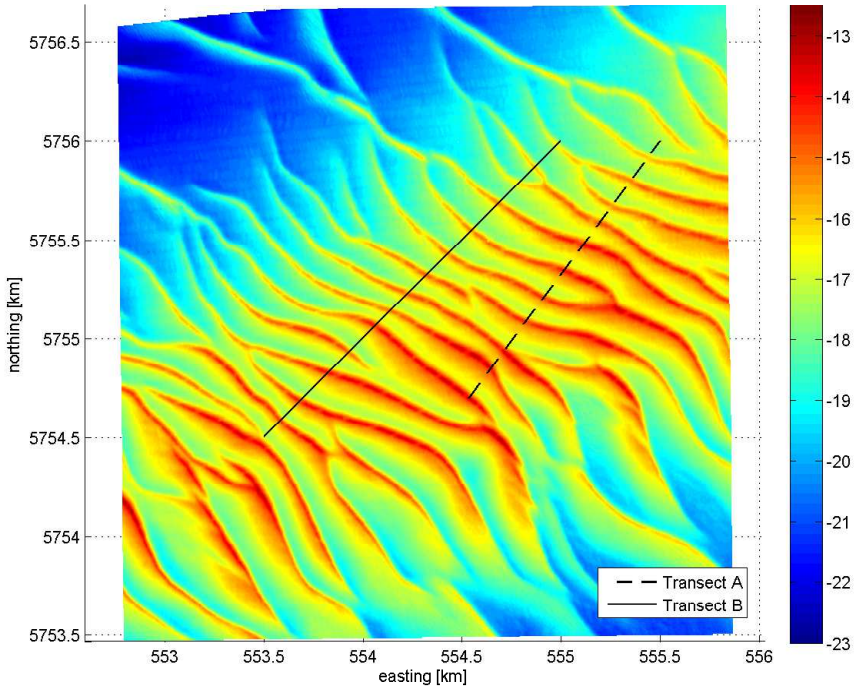

Figure 3.4: Location of the two intersections in the anchorage area. The sand wave numbering begins south east.

The model shows the wavelength from the different data in a graphic. From this point the minimum and maximum wavelength can be determined. Figure 3.5 shows a graphic of the data of 2011 from transect A, the power versus the wavelength. For Transect A a minimum wavelength of 63 metres and a maximum wavelength of 548 metres is chosen. The spectrum leads to smoothing the sea bed, which may result in a decreasing of the sand wave height. This is visible in Figure 3.6 were the difference between the Fourier analyse and the Real Data visible is. In the bottom figure the absolute height-difference is visible. The model gives also an error histogram, where the frequency of the difference in height is visible. This histogram is also a check to determine the right wavelength (Figure 3.7). The smaller the maximal and minimal range and the higher the frequency off zero, the smaller the error is. After eliminating all the other bed forms, the crest and trough points are selected. The model (Van Dijk et al., 2008) calculates:

- ▷ The wavelength, which is defined as the length segment connecting two consecutive troughs
- ▷ The sand wave height, which is defined as the line perpendicular tot the base line segment, connected to the selected crest points
- ▷ The assymetry index, which is defined as the ratio between the length of the toss- and lee side of the sand wave

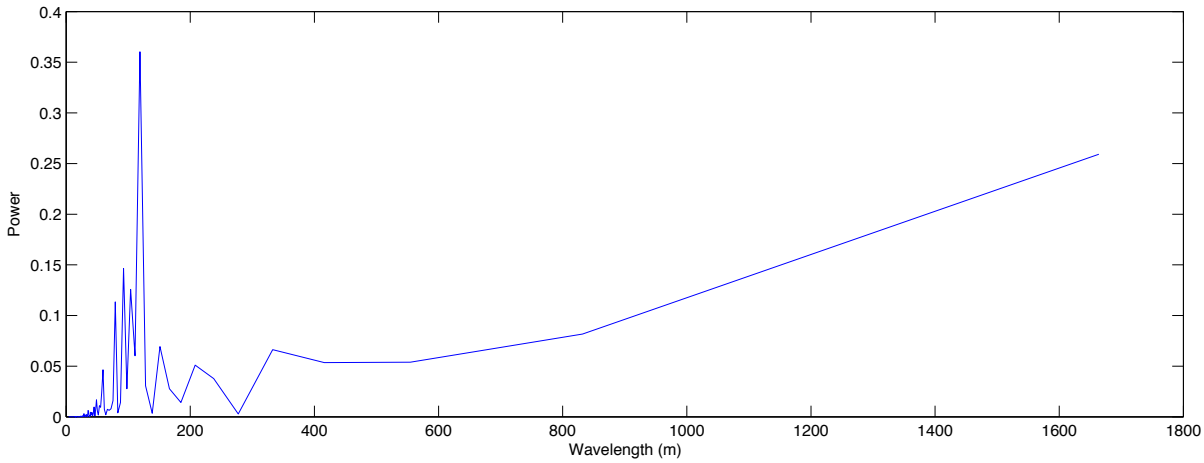

Figure 3.5: The different wavelengths and their powers, Transect A year 2011.

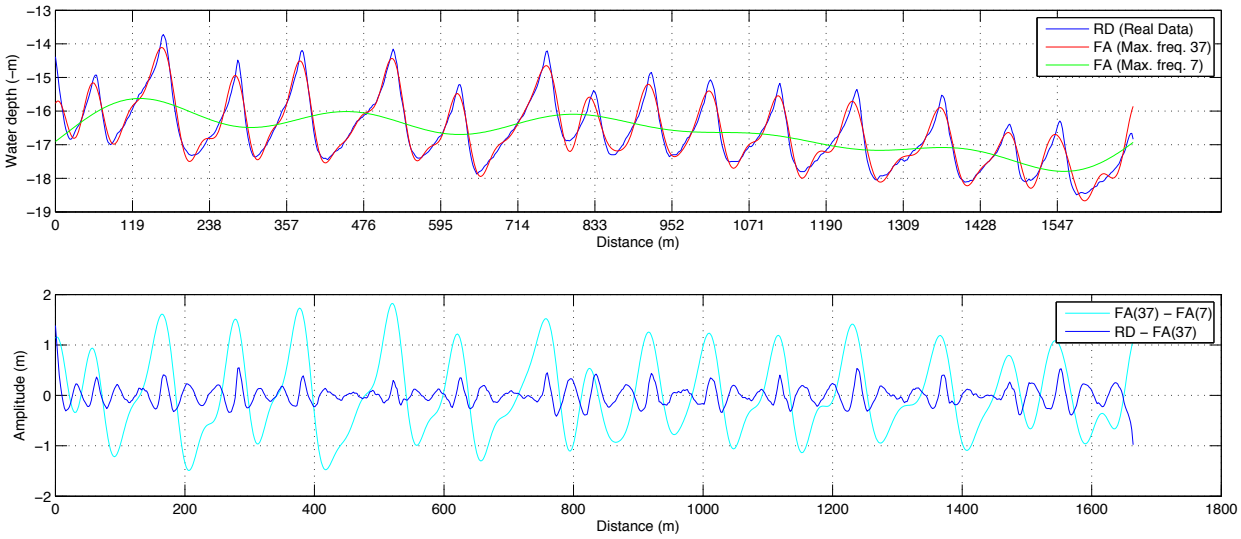

Figure 3.6: The Fourier analysis versus the real data, Transect A year 2011.

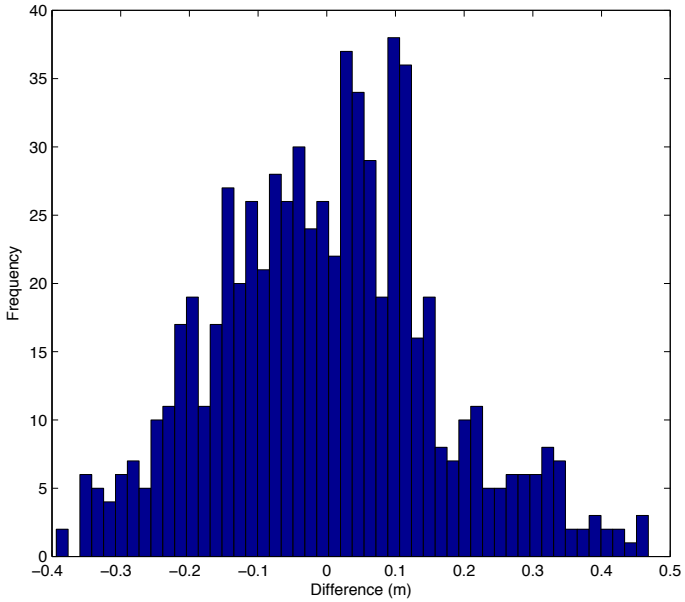

Figure 3.7: The error histogram of Transect A year 2011, with the frequency and the height difference between the original data and the fourier analysis.

The model selects the crest and trough points, next you have to confirm them manually. It is important that all bathymetric data sets use the same crest and trough points, otherwise the data is compared with other sand waves. This is also the case with the inflection points, which are also selected manually and used to determine the gradient of the sand waves. Figure 3.8a represent the manually selected crest and trough points for Transect A of data the set 2011 and Figure 3.8b for the inflection points.

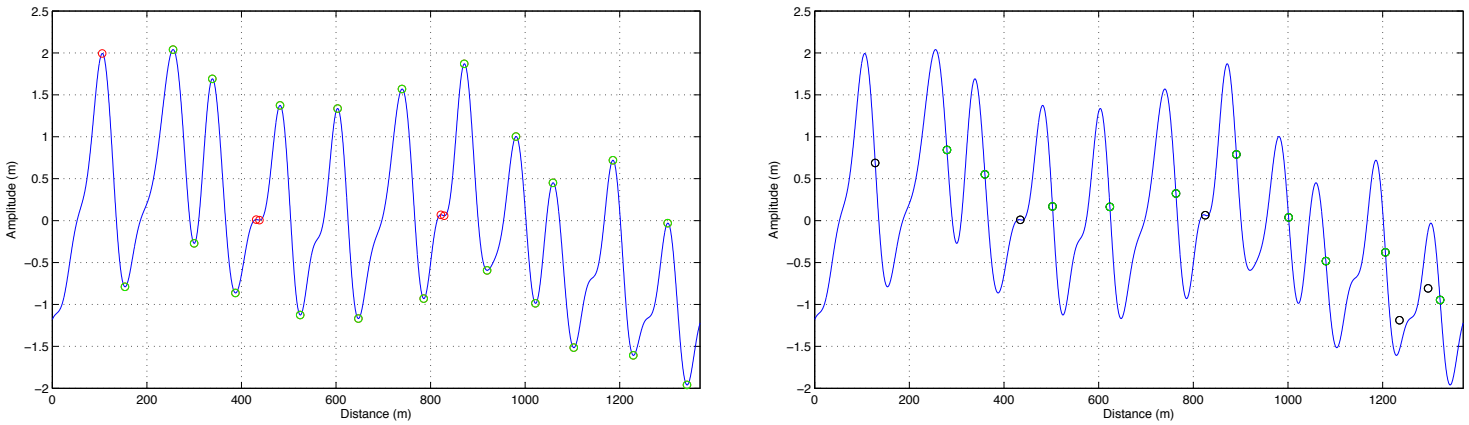

(a) (b)

Figure 3.8: Selecting the crest and through points, a green circle is a selected- and red a deselected Crest/Through point.(a) Selecting the inflections points, a green circle is a selected- and red a deselected Crest/Through point.(b) Both are represent Transect A, year 2011

When this analyse is done for all the different years along the transect, this allows us to determine the horizontal sand wave migration. This is done by linear regression, using the positions of the crest and troughs over the years. The regression coefficient represents the average migration rate in metres over a year for each crest and trough. It is interesting to see if there is a difference before and after the realisation of the sandpit. Therefore the migration rate between the data of HY06169-2 and HY08111-1 covers the 'before' stage and the migration rate between the data of 587-13 and HY14105 covers the 'after' stage. Also the migration rate is determined over all the available data sets.

To determine the uncertainty of the models a second transect is chosen, namely Transect B, which is also represented in Figure 3.4. This transect has a different angle and is situated on the edge of the sand wave field. Based on Figure 3.9 a minimum wavelength of 59 metres and a maximum wave length of 456 metres is chosen for Transect B. The calculated sand wave characteristics for each transect can be found in Appendix A.1.

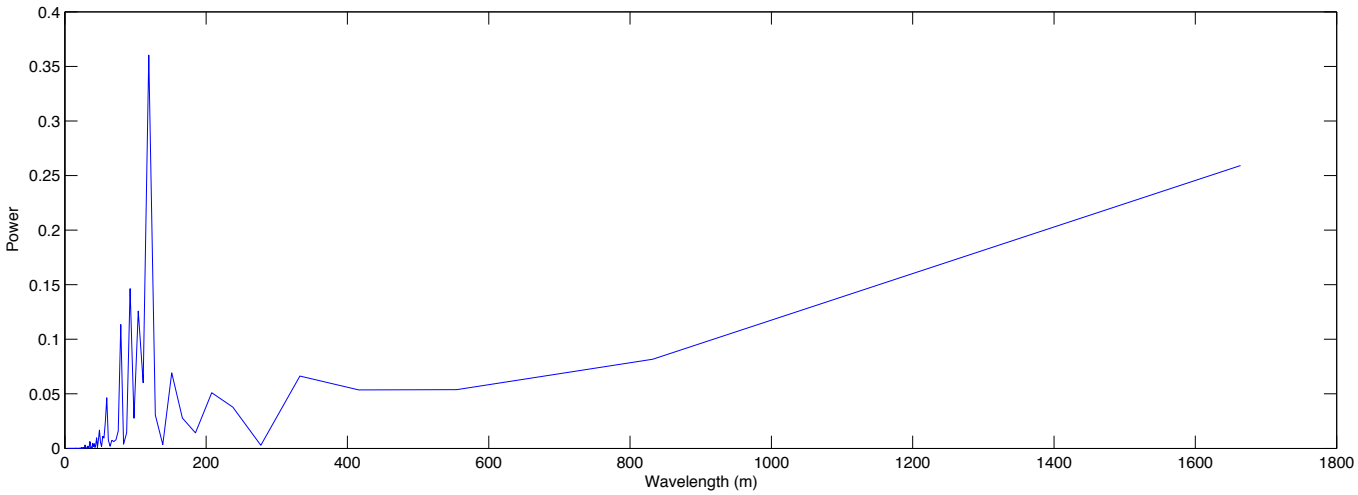

Figure 3.9: The different wavelengths and their powers, Transect B year 2011.

3.3.2. Migration rates from bathymetric data

The wavelength, height and ratio between the lee and toss side has been calculated for each transect. The results for every sand wave of both transects can be found in Appendix A.2. With the sand wave characteristics the migration rate can be determined by linear regression. The crest migration rates of the transects over the years are displayed in Figure 3.10 and 3.11.

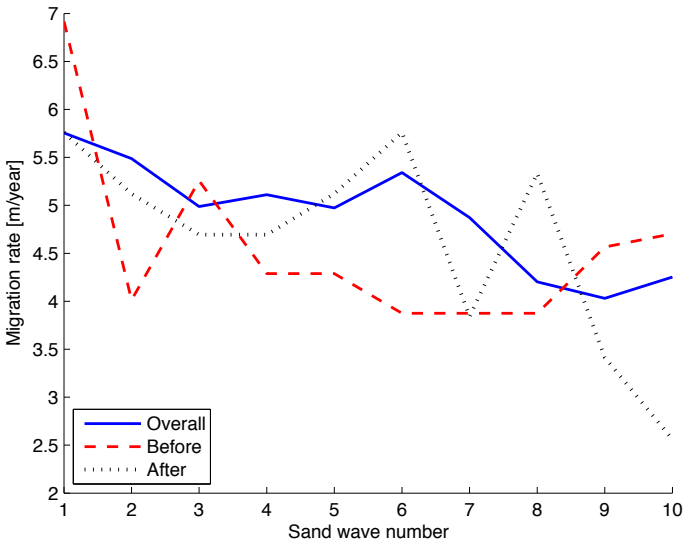

Figure 3.10: The migration rate for the different sand waves on Transect A.

In Figure 3.10 it is visible that the migration rate over all the years has a range between 5.9 and 4 meters a year. In the before stage the migration rate fluctuated between 3.9 metres and 6.9 metres a year. The migration rate at the after stage for Transect A fluctuates between 5.8 and 2.6 metres. The maximal difference is for both stages almost 3 metres, while this is larger than the calculated migration rate over all the years. Based on this numbers there is not a significantly difference between the before- and after stage.

When Transect B is taken into account, the same sand wave field, only a different orientation and more on the edge of the sand wave field, there is another pattern visible (Figure 3.11). The before stage fluctuates with the migration rate between 2.2 and 5.5 metres a year. The range is a little larger than Transect A, but also the migration rates are consequent lower. The after stage on the other hand has a migration range between 4.9 and 6.4 meters, which is considerably a smaller range and also higher than Transect A. Also it is striking that the after stage has always a larger migration rate and the before stage always have a smaller migration rate than the migration rate over the years.

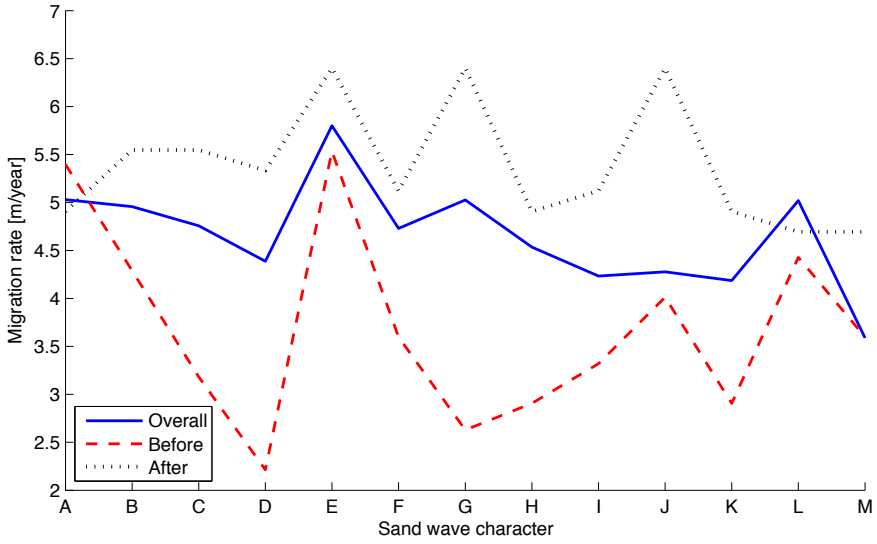

Figure 3.11: The migration rate for the different sand waves on Transect B.

The differences between both transects are considerably, while the migration rates are calculated for the same sand wave field. Both transects are illustrating that the place and orientation is very important to determine the migration. Selection of the a transect have a lot of uncertainty.

Because the migration of some sand waves are calculated by both transect, there is also a comparison made between the corresponding sand waves. This is shown in Table 3.2.

Table 3.2: Migration rates in metres per year for both transects (A and B). For the 'Overall', 'Before' and 'After' stage.

Sand wave number	**Sand wave character**	**A. Overall**	**B. Overall**	**A. Before**	**B. Before**	**A. After**	**B. After**
1	**F**	5.7	4.7	6.9	3.6	5.8	5.1
2	**G**	5.5	5	4	2.6	5.1	6.4
4	**I**	5.1	4.2	4.3	3.3	4.7	5.1
5	**J**	5	4.3	4.3	4	5.1	6.4
6	**K**	5.3	4.2	4.9	2.9	5.8	4.9

In Table 3.2 it is also visible that the migration values are very dynamic and there is not a relation between them. The position of the transect is therefore important and it is difficult to conclude what the migration rate of a sand wave field is.

Chapter 4

Model set up

The used models are described in this chapter. How the models work, but also the needed input is described. First an overview is given from the taken steps.
Figure 4.1 gives an overview over the used model applications and which input is needed.

The steps named briefly:

- First the bathymetric data is gathered from the sandpits. This data is used to generate the initial topography as input for the sandpit model.
- The predicted tidal velocity has to be transformed into several tidal components. How the transformation is done is described in subsection 4.1.2. After the transformation the values can be used as an input for the sandpit model.
- The sandpit model calculates the morphodynamic behaviour over the morphological times. The working of this model is briefly described in section 4.1.
- The output of the sandpit model is used as an input for the sand wave model. Before the output can be used it has to be transformed in the right formation by changing the velocity in tidal components.
- The grain size of the sediment is a new parameter and used as an input for the sand wave model.
- Eventually the output of both models together could determine the morphological behaviour of the sandpits and the sand wave characteristics in the surrounding area and in the sandpit.

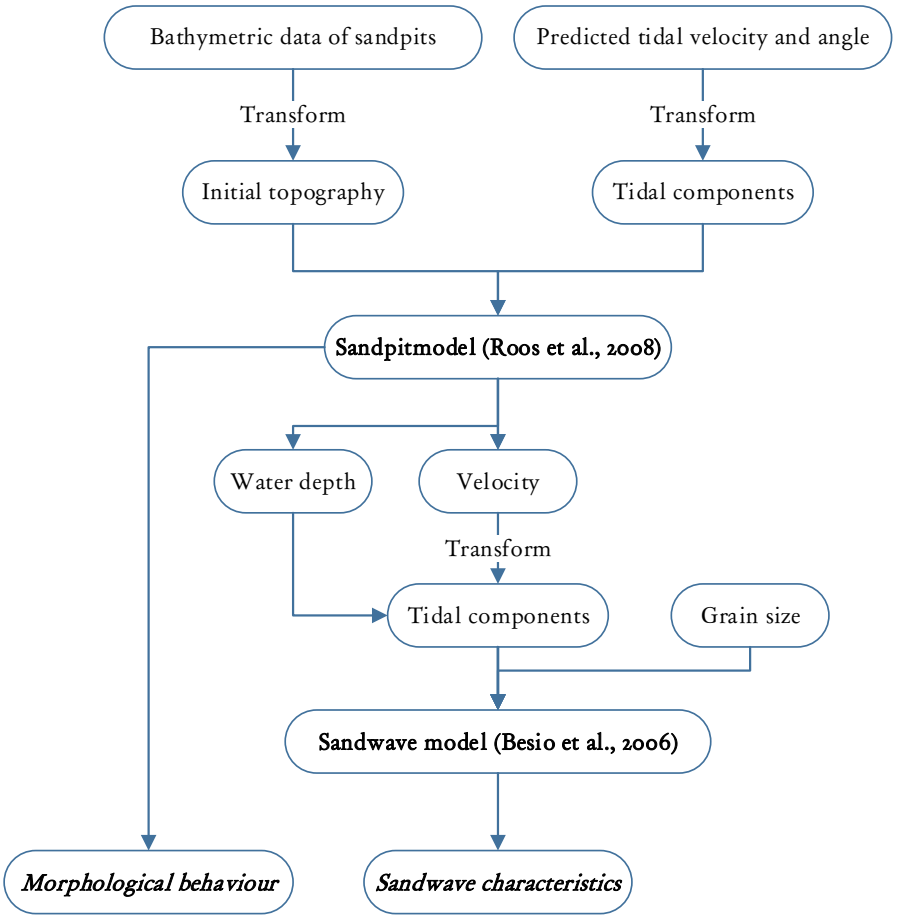

Figure 4.1: The steps which are taken in the model process.

4.1. Sandpit model

The sandpit model (Roos et al., 2008) is used to implement the current situation of the sandpits in the North Sea. The results show the morphodynamic effect on morphological scale. The velocity results will be used as input for the sand wave model. A brief description about the model will be given, which is important to interpret the results.

4.1.1. Description

The sandpit model is designed to investigate hydrodynamic effects and morphodynamic impact of large-scale offshore sand extraction, with a focus on the pit geometry. With this model the long-term impact of large-scale sand extraction on the morphology and tidal flow of the seabed can be studied. This includes the sandpit as well as its surroundings.

The model is based on an idealised process-based model of sandbanks from Hulscher et al. (1993). The first step is to define the pit geometry of the bathymetric data, the orientation angle, the flow velocity and the mean water depth. The boundary conditions with a spatial domain have to be specified and should be much larger than the length of the pit. The depth-averaged hydrodynamic model uses two-dimensional shallow water equations, including Coriolis effects and bottom friction. The basis equations are the conservation of momentum and mass and are expressed as:

$$g\frac{\partial \xi}{\partial x} + \frac{\partial u}{\partial t} + u\frac{\partial u}{\partial x} + v\frac{\partial u}{\partial y} - fv + \frac{\tau_{bx}}{\rho D} = 0 \tag{4.1}$$

$$g\frac{\partial \xi}{\partial y} + \frac{\partial v}{\partial t} + u\frac{\partial v}{\partial x} + v\frac{\partial v}{\partial y} - fu + \frac{\tau_{by}}{\rho D} = 0 \tag{4.2}$$

$$\frac{\partial D}{\partial t} + \frac{\partial Du}{\partial x} + \frac{\partial Dv}{\partial y} = 0 \tag{4.3}$$

here is $D = h + \zeta$ the total water depth, g the gravitational acceleration, u the depth averaged horizontal flow velocity, v the depth averaged vertical flow velocity, f the Coriolis parameter and τ_b the bottom friction vector.

Some assumptions of the model are:

- The effect of wind waves is neglected.
- The horizontal momentum dispersion is neglected.
- Chezy parameter is constant and uniform, i.e. the Chezy value is the same in- and outside the pit.
- Sediment, considered non-cohesive, is assumed to be transported as bed load mainly.
- A threshold for sediment motion is neglected.
- The contribution of the free surface displacement to the total water depth is neglected when the Froude number is assumed to be small.

The model has a quasi-stationary approach and has two time scales: a 'fast' hydrodynamic scale which refers to the tidal cycle and a 'slow' morphological scale which refers to the bed changes. The time scales are widely spaced, so the bed changes within a tidal cycle can be neglected. With all this information the transport formula and the bed evolution can be given by:

$$\vec{q} = \alpha|\vec{u}|^3 \left(\frac{\vec{u}}{|\vec{u}|} + \lambda \vec{\nabla} h \right), \frac{\partial h}{\partial t} = \vec{\nabla} \cdot \left\langle \vec{q} \right\rangle \tag{4.4}$$

This is including a downhill component. Here is α the proportionality coefficient in $m^{-1}s^2$, λ the dimensionless bed slope coefficient, $\vec{q} = (q_x, q_y)$ the volumetric sediment flux in m^2s^{-1}, $u = (u, v)$ the flow velocity vector in x- and y-direction, h the water depth, t the morphological time coordinate, ∇ represents nabla-operator and the angle brackets denote averaging over a tidal cycle.

It is possible to calculate with different flow conditions, these conditions can be determined by the linear friction coefficient, phase lag and the several currents with the following Formula (4.5):

$$J(t) = M_0 + M_2 \cos \omega t + M_4 \cos(2\omega t - \varphi) \tag{4.5}$$

It represents a unidirectional tide along the x-axis with a residual component M_0, a semi-diurnal lunar component of amplitude M_2 and its overtide (amplitude M_4, phase lag φ).

The model uses a spatial periodicity in x- and y- direction, to determine the spatial domain, the minimum wave number in the Fourier expansion has to be set. The relationship is explained by $L_{space} = \frac{2\pi}{k_{min}}$. In this case the k_{min} is 2.45×10^{-4}. This corresponds with a spatial domain of 25.6 kilometres. In simple words the model is constructed on a chessboard, on every box a pit is situated. It is important to choose a size of the box, that the pits on the board will not influence each other. Otherwise the results are not only influenced by one pit, but several.

The model output consists of seabed topography, time-dependent flow patterns and surface elevation. The results can indicate the position of the pit, its centre of mass and the area of morphodynamic influence. For this research it is useful to look into the pit, at the surroundings and at the location where the data research is done.
Some drawbacks to use the model for the specific Maasvlakte 2 case:

- The model uses an uniform depth outside the pits, which means that the assumption is a flat bottom. In the North Sea this is not the case. The little perturbation at the bottom are eventually flatten out by the long-term modelling, but an overall gradient at the seabed is therefore neglected.
- The model uses only one roughness value, while the grain size differs, especially the difference between the grain size in the pit and outside the pit.
- The model is linear in the bed amplitude which is valid for shallow pits, while in this case the pits are not shallow at all.

4.1.2. Input

To give a realistic view on the results, the input for the model is important. The input is based on the tidal current and the geometry of the sandpits, which should have the shape of the realised sandpit for Maasvlakte 2.

Tides

The tidal flow is very important for the model, these tides cause the velocity and direction of the flow, which determines the displacement of the sediment. The tidal flow in the model is described with Equation 4.5. The Hydrographic Service of The Netherlands Navy also calculates the velocity of the flow caused by the sea. The calculation is determined by the observations from different tidal measurements, which are monitored the whole year. The flow velocity is based on hydrodynamic model simulations and the predicted velocities are published in the HP33 (Dienst der Hydrografie, 2013). The predicted velocities are calculated in the first fifth (from the seven) layers of the water column. This means that lower part of the column, situated at the sea bed, is not included in the prediction.

The program NL tides (The Netherlands Hydrographic Service, 2013) is a digital version of the HP33, which show the predicted velocity and direction of the flow with a maximum frequency of 5 minutes. A total spring neap cycle is gathered for each season. With the program t_tide of Pawlowicz et al. (2002) this spring neap cycle signal can be divided, by means of a Fourier analysis, in a M2, M4 and M6- signal. Because the sandpit model deals with M0, M2 and M4, only these information is taken into account.

Because the differences in season were not large, the season spring is chosen as initial condition. The differences in the season is described in Appendix B, where also a larger explanation of the used method is given. The t_tide results of the related tidal ellipse is shown in Figure 4.2. The sand pit model, as it is implemented, can only handle (as seen in Eq. 4.5) a bi-directional M2-tide and a M4-tide with a phase difference with respect to the M2- velocity. So M0 and both ellipses M2 and M4 must be projected on the major axis of the M2-ellipse. In this way a vector arises, Table 4.1 gives an overview of the values for the phase and amplitude of the tidal components.

Table 4.1: Velocity and phase on the major axis of the M2 tidal flow.

	Velocity [m/s]	**Phase** [°]
M0	0.053	–
M2	0.746	321
M4	0.053	299

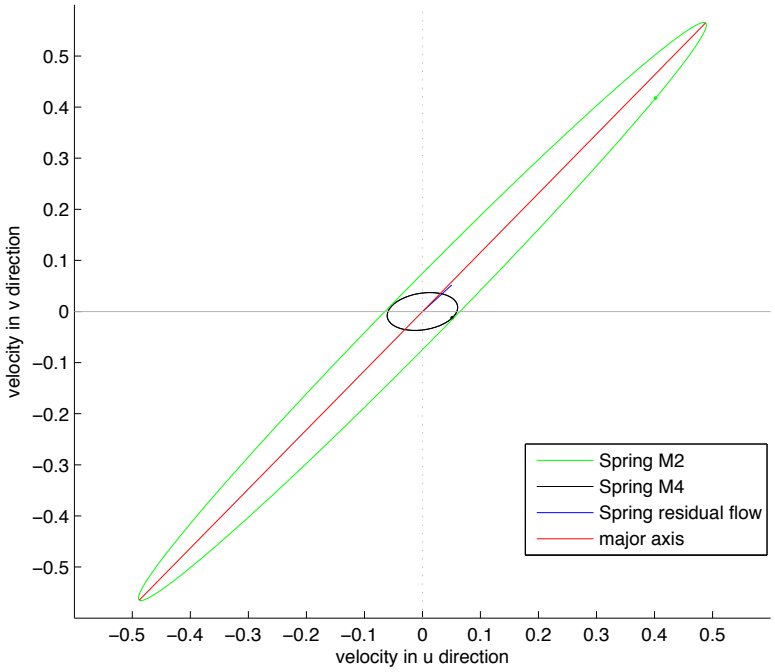

Figure 4.2: The tidal spring tide, the residual is very small and almost invisible by the major axis.

In AppendixB the transformation from an ellipse to a major axis and the tidal flow versus the used flow in the model is shown. A translation in time is needed to eliminate the phase from Equation 4.6 and arrive at Equation 4.5.

The amplitudes stay the same, only the phase difference (φ) will be 39°. Figure 4.3 illustrates the difference between $\hat{J}(t)$ and $J(t)$. The signals are the same (inclusive the amplitude), only the starting time is different (phase).

Eventually the model calculates the velocities patterns on a fixed location. The translation for the output of the sandpit model into the used velocity for the sand wave model is described in Appendix B.

$$\begin{gathered} \hat{J}(t) = M_0 + M_2 \cos(\omega t - \varphi_{M2}) + M_4 \cos(2\omega t - \varphi_{M4}) \\ \text{with:} \\ \varphi = 2\varphi_{M2} + \varphi_{M4} \end{gathered} \tag{4.6}$$

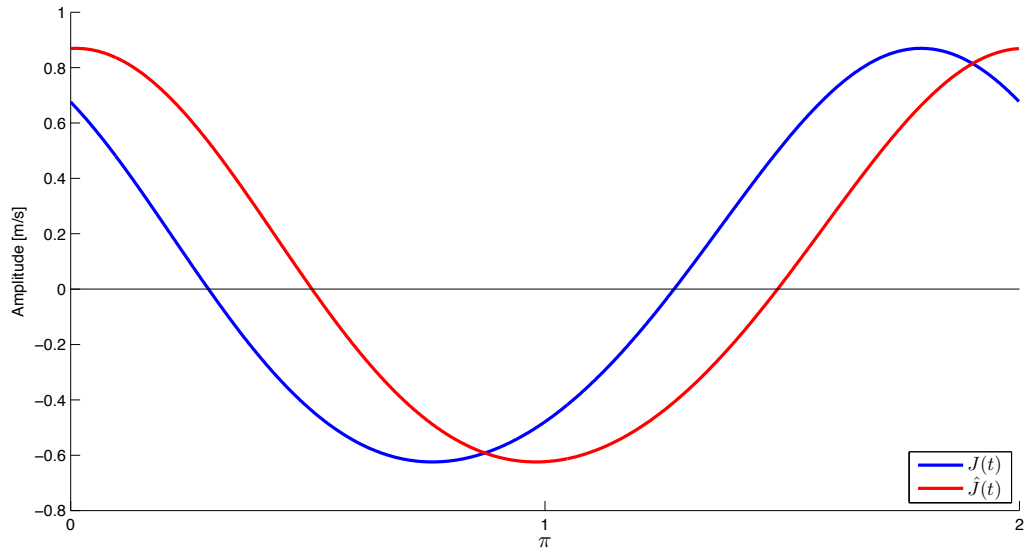

Figure 4.3: The tidal flow J(t) versus J($\hat{t}$) on the M2 major axis with a period of the total spring neap cycle.

`Sandpit`

The two sandpits of the Maasvlakte 2 have to be implemented in the model. The detailed pit geometries are gathered from bathymetric surveys of the Hydrographic Service of the Royal Netherlands Navy. The bathymetric survey is done in 2012 and the grid size of the data is 3- by 5- metres, in x- and y- direction. Because the sandpits have a large surface area not all data points can be implemented, otherwise the dataset becomes too big. Therefore the data is transformed into a 100- by 100- metres grid. Figure 4.4 illustrates the differences for both grids when taken an intersection. The differences in the intersection is that the seabed is more smooth. Small-scale details are not relevant for the model and therefore not a problem.

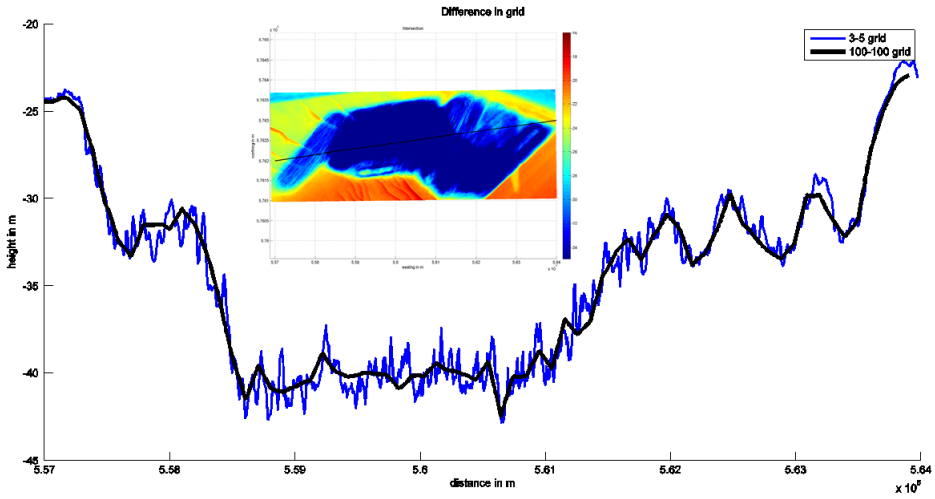

Figure 4.4: The difference between the grids, also the place of the intersection is visible

As already stated in the model description (section 4.1.1), the seabed around the pit has to be flat. However, in reality the seabed is not uniform and has a slope. Figure 4.5 gives an overview with the different ranges in depth of the sea bottom around the pits. The non-uniform depth makes it difficult to put the pits into the model, so the little pit is 'cut' out and shifted to the same surrounding depth as the biggest sandpit. In this way a small bit of data of the smallest sandpit has been lost, but not significantly.

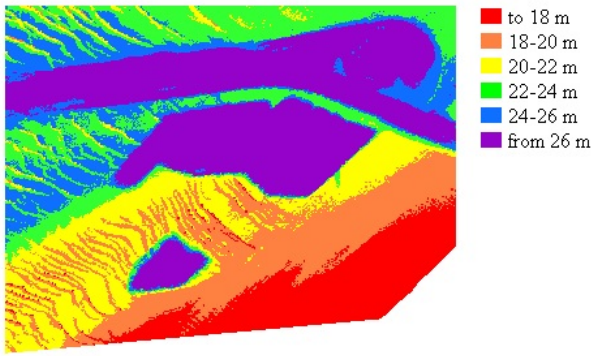

Figure 4.5: The depth ranges given in colours

Besides the x-axis of the model is aligned with the dominant flow direction, the pits have to be rotated in the angle of the dominant flow to modelling the case. Figure 4.6 illustrates the final pits; the correct scale, a flat seabed, the idealised small sandpit and the rotated situation. At first the navigation channel is not implemented in the model.

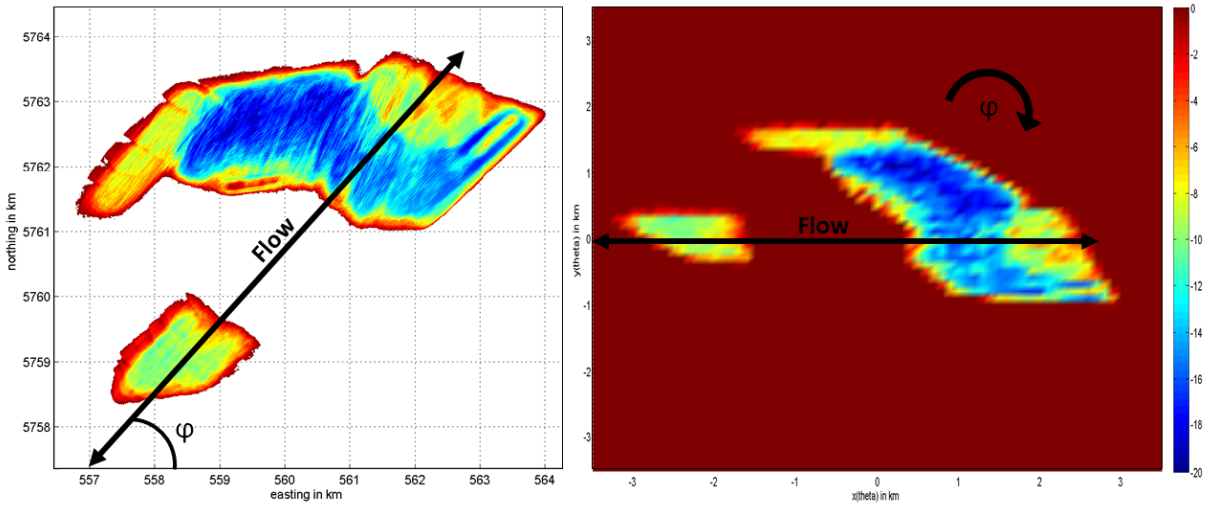

Figure 4.6: Left the original pit (shifted little pit) and right the modelled pits with rotation and a grid of 100- by 100- m

4.2. Sand wave model

The sand wave model Besio et al. (2006) is used to study the sand wave characteristics in the surrounding area of the modelled sandpit. The model is a linear stability-based model and based on the physical equations for conservation of motion, but assumes idealized and simplified conditions (Dodd et al., 2003). The model can be used to predict the initial formation of the sand waves, but is not able to predict the long-term formation processes. Therefore the input from the sandpit model is used, to still get insight of the changes on the long-term time scale. The model predicts the conditions leading to the appearance of both tidal sand waves and sand banks and determines their main geometrical characteristics. The model is based on the study of the stability of the flat seabed configuration. This is done by considering small seabed perturbations and providing linear analysis of their growth. The input is based on the velocity and water depth, which is generated from output of the sandpit model. Also the grain size is an important factor. These inputs are discussed in the following paragraphs.

4.2.1. Input

The water depth is generated from the output of the sandpit model. The positions of the local depths are discussed in Chapter 5.

Velocity

The sandpit model calculates the flow velocity, as given in Equation B.1 and B.2. The output is given in real- and imationair- tidal components. This is due to complex bed amplitude, where the growth rate has a complex quantity. The imagitonary part of the growth rate is associated with migration. And has to be solved by time dependent Fourier components, where among other the velocity is included. A translation is needed to use the flow velocity as input for the sand wave model. This translation is described in Appendix B. Only the amplitude of the M2 velocity component is used in the sand wave model, because this is the dominant flow velocity.

Grain size

Also the grain size is important to determine the sand wave characteristics. From Van Tongeren (2013) data is gathered at the surroundings and in the pit for several years. This data is used to come to one uniform grain size. More than 50% of the studied sediment was present in the range from 250-500 μm, therefore the grain size of 375μm is chosen. This value is used for all locations, because it is difficult to coordinate to the right location in combination with the correct data.

4.3. Output

The sand wave model calculates whether the circumstances are present to form sand waves and if so it calculates the preferred wavelength, growth rate and wave numbers in both x- and y-direction. With these outputs the response time of the sand wave can be calculated with the following formula (Cherlet et al., 2007):

$$\begin{aligned} T_r^* &= \frac{(1-p_{or})\sqrt{\psi_d}}{\Gamma_r d^* \omega} \\ &with: \\ d^* &= \frac{d}{h_0} \\ \psi_d &= \frac{(\omega h_0)^2}{(\rho_s/\rho - 1)gd} \end{aligned} \tag{4.7}$$

Where Γ_r is the dimensionless growth rate, ω the angular frequency of the tide in rad/s, P_{or} the sediment porosity, d the grain size of the sediment in meters, h_o the main water depth in meters, d^* the dimensionless grain size, ψ_d the mobility number, ρ_s the sediment density and ρ the water density both in kg/m^3. The used parameters are shown in Table 4.2.

Table 4.2: Parameters for the sand wave model.

d	ρ_s	ρ	g	p_{or}	ω
$[m]$	$[kg/m^3]$	$[kg/m^3]$	$g[m/s^2]$	-	$[rad/s]$
375 10^{-6}	2650	1020	9.81	0.6	1.14 10^{-4}

Chapter 5

Results

In this chapter the results of the model study are shown. The first part describes the results of the evolution of sandpits over the years. These results are used as input for the sand wave model. Also those results are shown and a comparison is made for the sand wave characteristics with- and without the sandpits implemented. Finally the results are given from the sandpit model where the navigation channel is implemented. The model setup has already been explained in Chapter 4.

5.1. Sandpit morphodynamic evolution

In Figure 5.1 the results of the evolution of the pits are shown for a period of 10, 30, 50, 100, 150 and 200 years. From the figures the following conclusions can be made: i) the pits will migrate in the direction of the dominant flow (the positive x-axis), ii) the pits become shallower, iii) the slopes of the pits will flatten out, iv) at the side of the large pit shallow areas will appear and v) the small pit will move to the large pit and finally merge into the large pit.

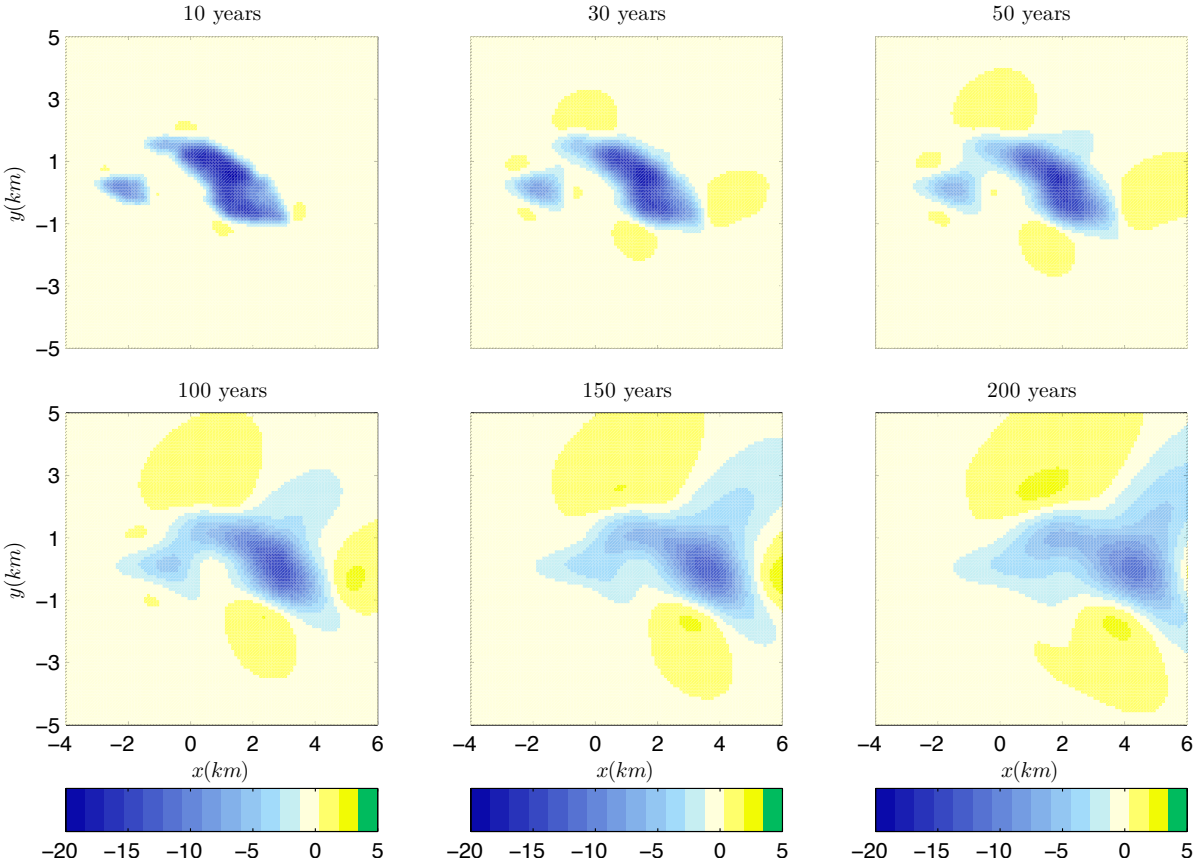

Figure 5.1: The morphological behaviour of the pit over time

Migration of the sandpits

As shown in Figure 5.1 both pits migrate in the direction of the tidal flow. This is caused by the asymmetry of the forcing. To determine the migration three transects are taken and visible (G,H,I) in Figure 5.2. The migration rate is determined by following the deepest point on the transect (see Figure 5.3 to 5.5). Because Transect G and I are aligned in the same direction, those are illustrated in the same figure.

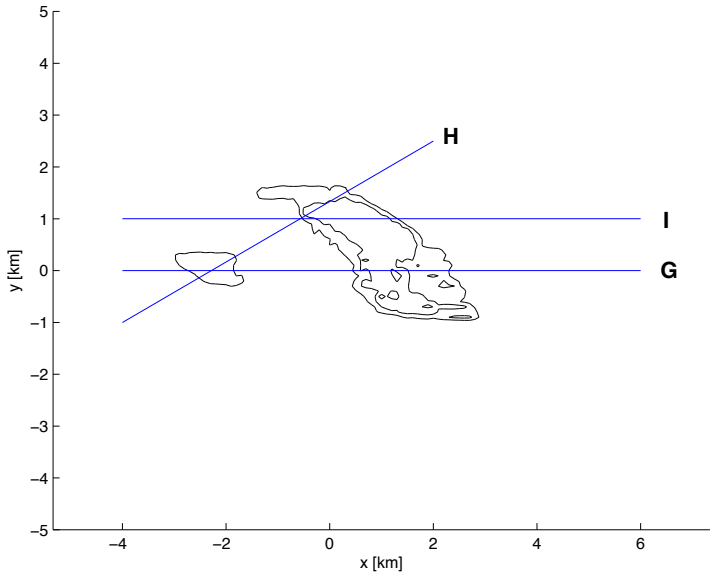

Figure 5.2: The location of the transects (G,H and I)

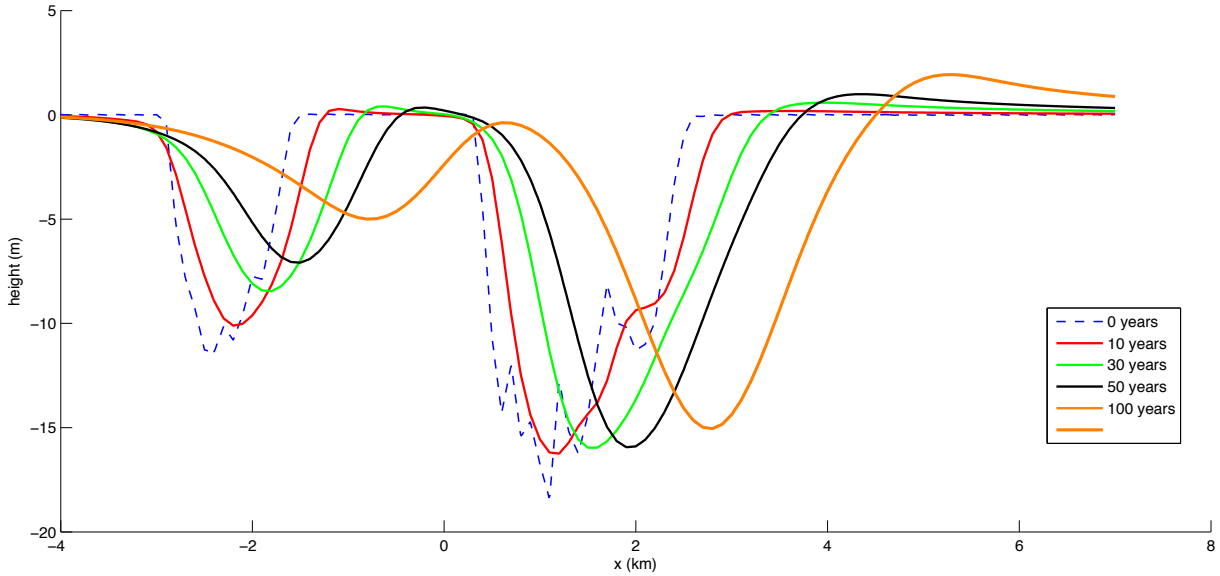

Figure 5.3: Transect G

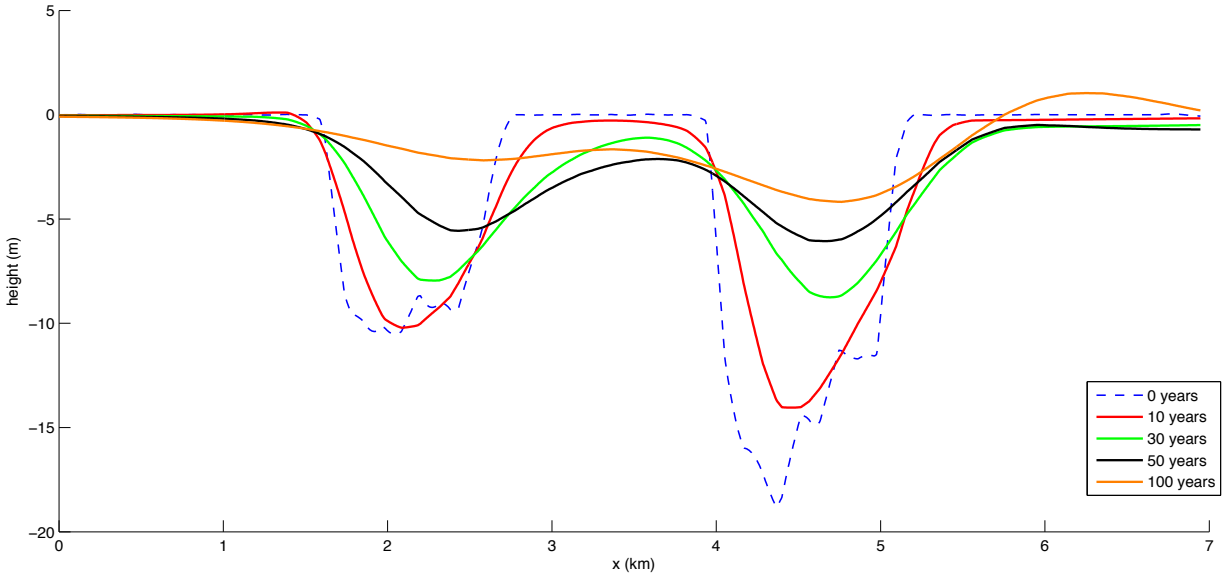

Figure 5.4: Transect H

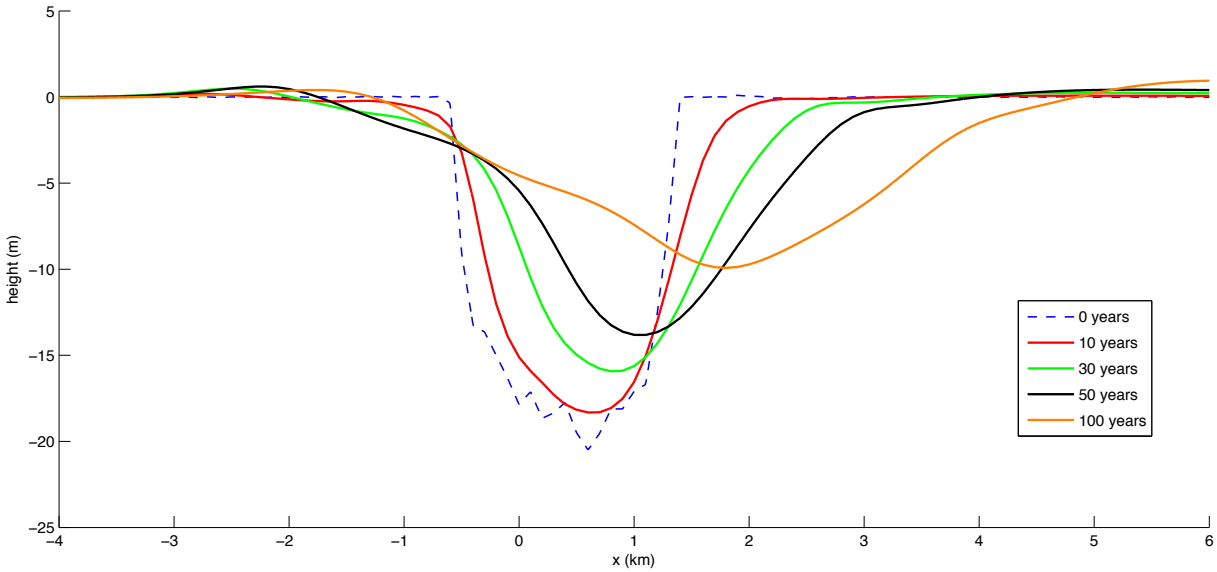

Figure 5.5: Transect I

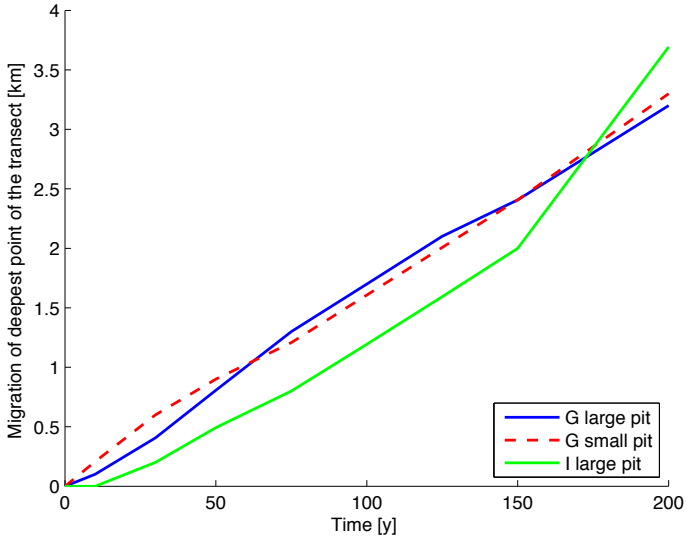

Figure 5.6: The absolute migration of the pits from Transect G and I over time

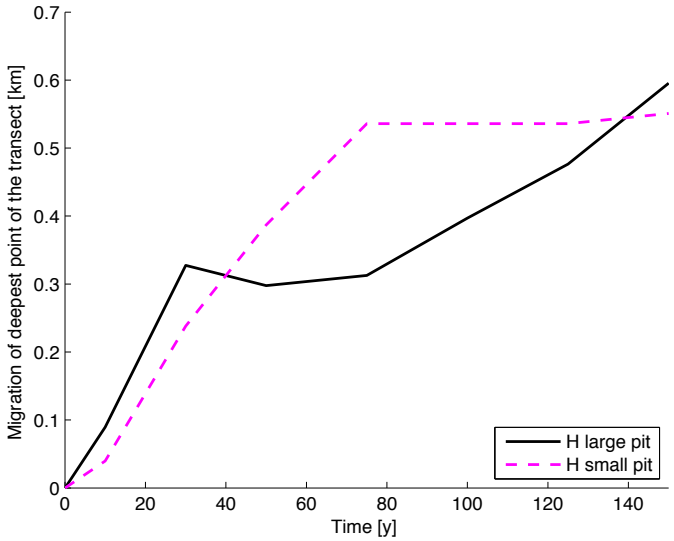

Figure 5.7: The absolute migration of the pits from Transect H over time

The small pit migrates faster in the first 10 years than the larger pit. This is possible caused by higher flow velocity in the smaller pit, due to a lower water depth. Eventually the smaller and larger pit will migrate almost with the same distance. That the migration of Transect H is lower is caused by a different direction of the transect. This concludes that the deepest point of the pit not only move in the positive x-direction but also in the y-direction.

Also the migration rate in m/year between the modelled years is given in Figure 5.8 and 5.9. These results show that the migration rate of the deepest point of the pit is not stable. The highest migration rate takes place in the first years, then the migration rate will decrease and finally becomes stable for some years. The migration rate of Transect I between 150 and 200 years is very high, the reason is of this is the large pit becomes more shallow and the deepest point is flatten out. This is visible in 5.5.

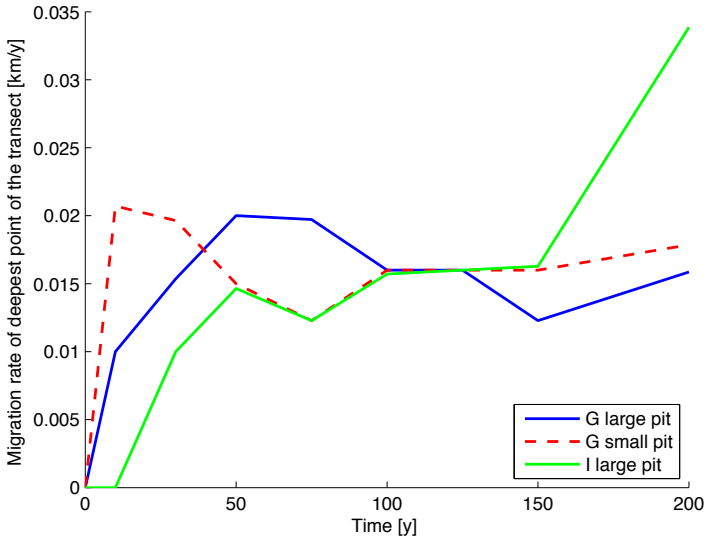

Figure 5.8: The migration rate of the pits from Transect G and I in m/year

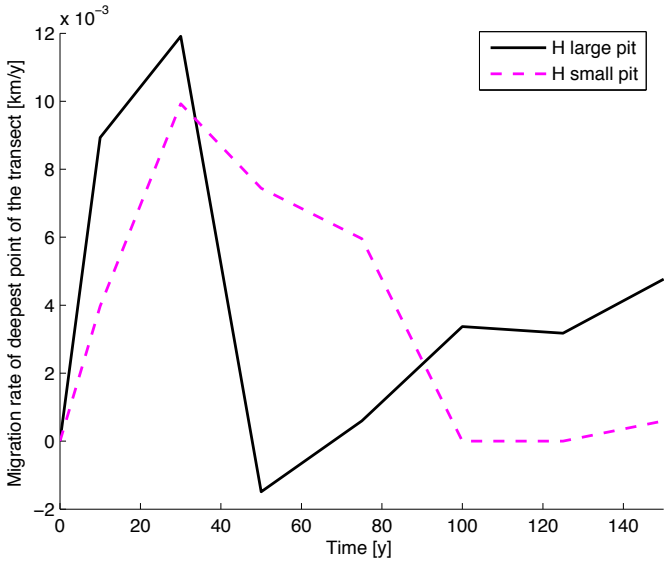

Figure 5.9: The migration rate of the pits from Transect H in m/year

`Edges flatten out`

Due to the larger flow velocity at the surroundings of the pits the sediment at the seabed become in motion and is transported into the pit. In the pit the flow velocity will decrease, the sediment will settle down and the pit becomes shallower, which is shown in Figure 5.10. In this figure $\frac{dh}{d\tau}$ is given over the years. (τ) stands for the morphological time, in other words $\frac{dh}{d\tau}$ is the difference in depth during the change of morphological time. Through the years the erosion and sedimentation is decreasing, this is due to decrease of the relative impact of the sandpit on the flow. The influence of the pit on the flow will decrease and so will the flow influence the pit, it is a downward spiral.

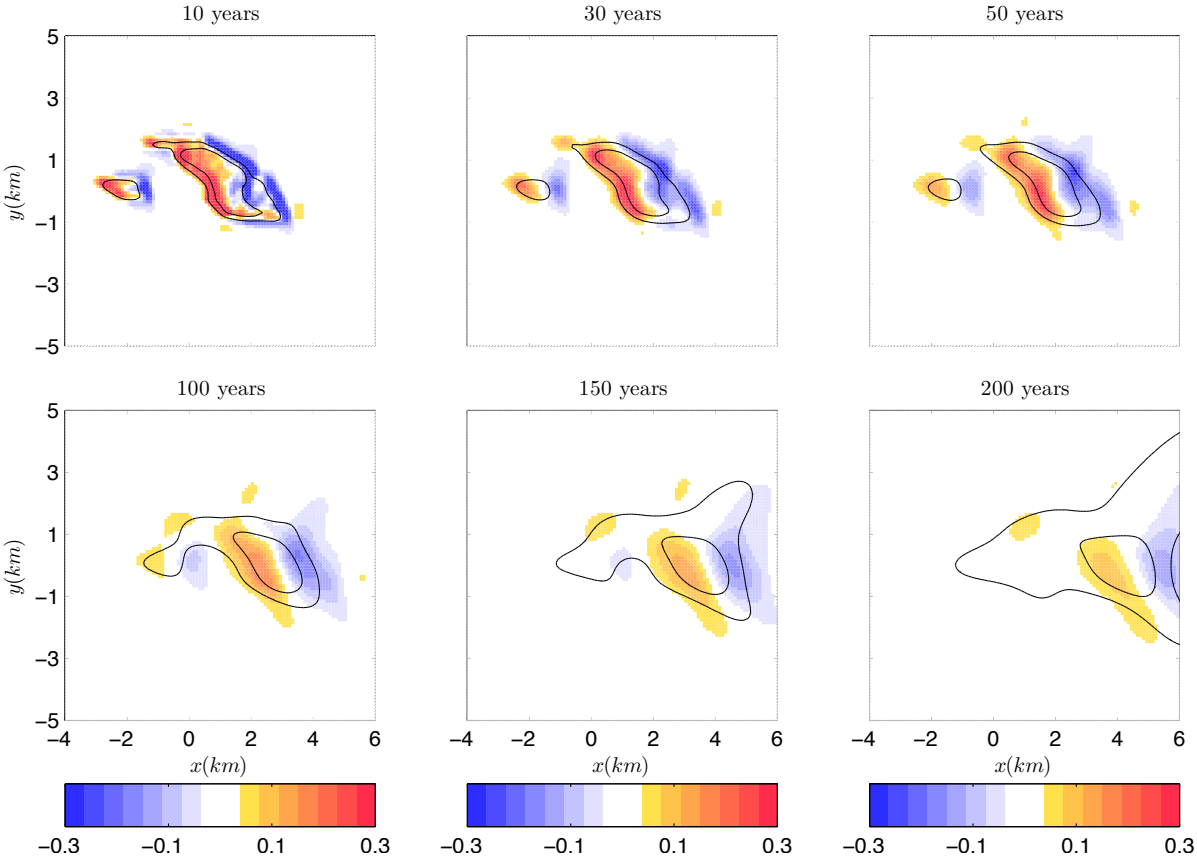

Figure 5.10: The $\frac{dh}{d\tau}$ for 10 to 200 years

Depth of the sandpits

Figure 5.11 shows a graphic for the different depths of the transect for the deepest depth for each modelled year. For all the pits and transects the depth is increasing, first fast and after a while slower. Take into account that this not the deepest depth of whole the pit, but only for the transect.

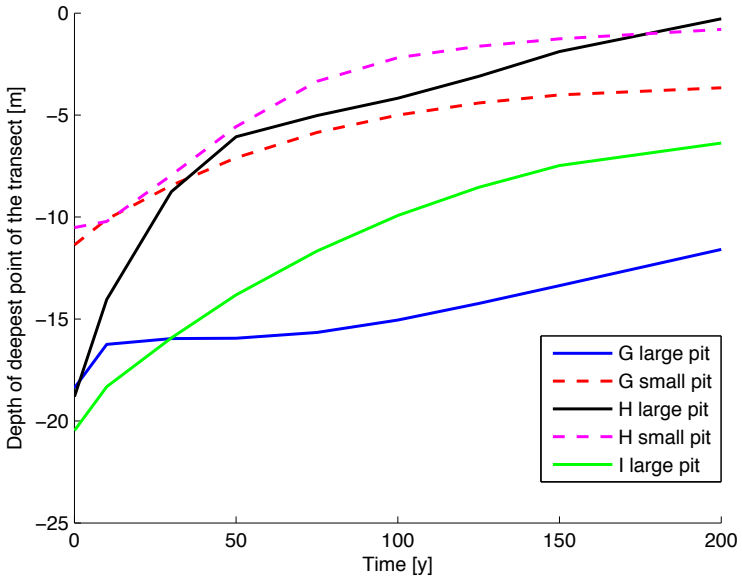

Figure 5.11: The maximal depth of the Transects G,H and I over time

The border between sedimentation and erosion is present on the edge of the pit. Because the velocity is changing by the water depth of the pit. On one side the edge it is eroding on the other side it is settling. The slopes are flatting out and become less steep. This is visible by Transect G, H and I in Figure 5.8-10, where the different seabed level are visible through the years.

5.2. Sand wave characteristics

For the sand wave characteristics the initial situation at the surrounded area is calculated, this is done before the pit is implemented. In this way the influence of the pit is better visible. The initial conditions are the same conditions as used as input for the sandpit model. For the sand wave model a depth of 24 metres is used. Because the M2 is the dominant tidal velocity, a value of 0.7742 m/s, equal to the amplitude of M2, will be used in the calculations. The grain size is chosen uniform for all locations, namely 375 μm. (Rijkswaterstaat, 2013).

This calculation gives the following results: a wavelength of 376 metres, a growth rate of 0.05 and a sand wave response time of 7.7 years. This response time corresponds with the most dynamic sand wave field in the Belgian Continental Shelf, the Westerhinder, following Cherlet et al. (2007).

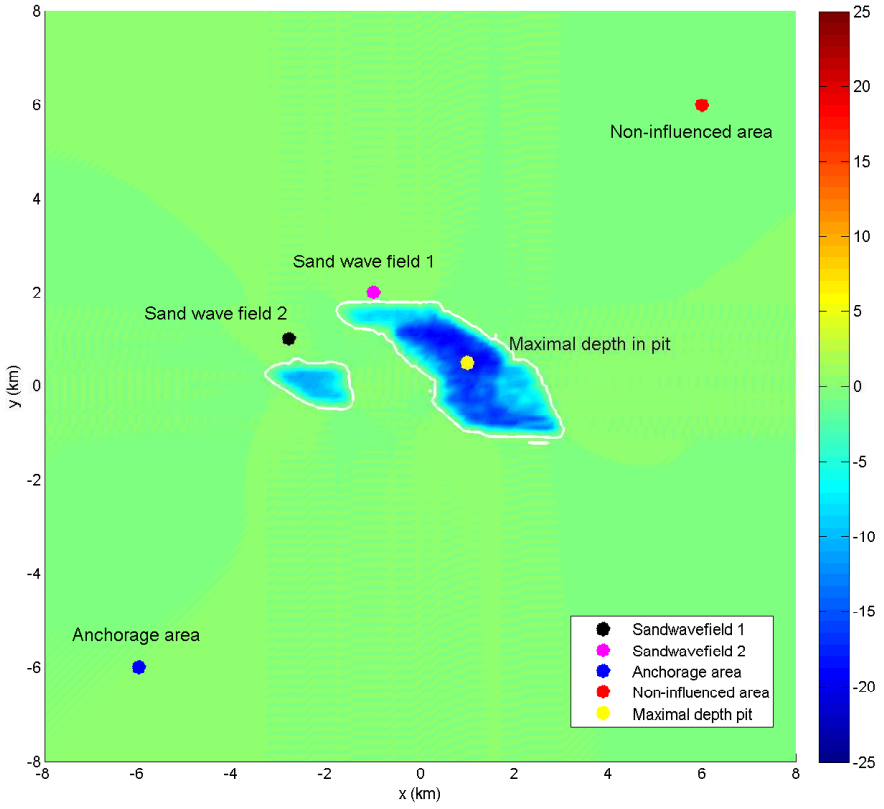

Figure 5.12: The locations of the different positions which are evaluated.

To study the influence of the sand wave characteristics five locations are chosen. The locations are shown in Figure 3.2. Based on the most dynamic areas in combination with the sand wave fields at the west side of the pits, position 1 and 2 are chosen. The third location is situated in the anchorage area. Location four is the no-influence area described by Klein and van den Boomgaard (2013) and finally for the fifth location a position in the deeper part of the pit is chosen.

For each position the results of the sandpit model and the sand wave model will be discussed. In Appendix C tables can be found of the tidal amplitudes, depth, growth rate, wave length and response time for every location. In the next paragraphs only textual explanation is present and for each location a small table of the output for the initial condition, 10, 50 and 100 years.

Sand wave field 1 Through the years the residual velocity (M0=0.062) will increase with a maximum of 14%, while the M2 velocity amplitude and depth stay, with a maximum deviation of 2%, almost the same. This corresponds with small changes over the years, which is visible in the sand wave characteristics. The sand wave lengths are around 377 metres, the growth rate 0.05 and the response time is 6.6 to 7.5 years, which is lower than the initial condition. In this period the orientation of the sand waves will change 2 ° to the South.

Table 5.1: The sand wave characteristics at the location 'Sand wave field 1'

τ	θ	M_0	M_2	M_4	$\widetilde{\varphi}_{M4}$	h_0	Γ_r	L
years	[°]	[m/s]	[m/s]	[m/s]	[°]	[m]	[-]	[m]
Initial	90	0.072	0.744	0.053	321	24.0	0.05	376
10	92	0.064	0.758	0.060	318	24.0	0.05	375
50	92	0.067	0.766	0.060	324	24.0	0.06	379
100	91	0.069	0.761	0.059	324	24.0	0.05	375

Sand wave field 2 Compared to sand wave field 1 this field has the same influence but the residual velocity is higher (M0= 0.069 m/s), with an increasing up to 9%. Furthermore not a lot of differences appear between the two fields; the magnitude of the values are almost the same and the wave lengths of field 2 are approximately 372 metres. The response time of field 2 is higher, but still has the same magnitude; 6.9 to 8.8 years. The orientation of the sand waves changes 5 ° to the South, which will reduce to 2 ° South.

Table 5.2: The sand wave characteristics at the location 'Sand wave field 2'

τ	θ	M_0	M_2	M_4	$\widetilde{\varphi}_{M4}$	h_0	Γ_r	L
years	[°]	[m/s]	[m/s]	[m/s]	[°]	[m]	[-]	[m]
Initial	90	0.072	0.744	0.053	321	24.0	0.05	376
10	95	0.070	0.725	0.053	321	23.8	0.04	369
50	94	0.072	0.743	0.054	321	23.7	0.05	373
100	93	0.073	0.753	0.055	321	23.9	0.05	371

Anchorage area The location of the anchorage area is further away from the sandpits than the sand wave fields, this could mean that the influence of the pits is lower. The lower effect is visible in the residual flow, M2 amplitude and the depth, all are not changing significant. This causes also no changes in the wavelength of 375 metres and a growth rate of 0.05. The response time has the same magnitude as both sand wave fields, which means that the anchorage area behaves like a sand wave field. The response time is therefore steady and the sand waves will keep the same orientation as the original situation.

Table 5.3: The sand wave characteristics at the location 'Anchorage area'

τ	θ	M_0	M_2	M_4	$\widetilde{\varphi}_{M4}$	h_0	Γ_r	L
years	[°]	[m/s]	[m/s]	[m/s]	[°]	[m]	[-]	[m]
Initial	90	0.072	0.744	0.053	321	24.0	0.05	376
10	90	0.072	0.743	0.053	321	23.8	0.05	376
50	90	0.072	0.743	0.053	321	23.7	0.05	376
100	90	0.072	0.744	0.053	321	23.5	0.05	376

Non-influenced area The non-influenced area has the same distance from the pits as the anchorage area, it is expected that the influences here are not significant. However, in this area there are more fluctuations visible than in the anchorage area. Following Klein and van den Boomgaard (2013) this was not an influenced area and as shown in Figure 1.2 there were no sand waves presented. This means that in the area 'new' sand waves and more influences will occur than expected. The residual flow will decrease, while at the other locations it is increasing. The response time will grow and has the same magnitude as the sand wave fields, from 7.8 to 9 years. The sand waves will keep the same orientation as in the initial condition.

Table 5.4: The sand wave characteristics at the location 'Non-influenced area'

τ	θ	M_0	M_2	M_4	$\widetilde{\varphi}_{M4}$	h_0	Γ_r	L
years	[°]	[m/s]	[m/s]	[m/s]	[°]	[m]	[-]	[m]
Initial	90	0.072	0.744	0.053	321	24.0	0.05	376
10	89	0.071	0.742	0.054	321	24.0	0.05	376
50	89	0.070	0.739	0.054	321	24.1	0.05	374
100	89	0.068	0.732	0.054	321	24.3	0.05	372

Maximum depth in pit The largest depth in the pit has not a fixed position, it changes with the migration of the pit. The x- and y-position is given in the table from the largest depth in the pit over the years (Table 5.5). The residual flow and M2 amplitude is increasing, while the depth is decreasing. It is expected that a decreasing depth will cause an increase of the velocity. During a period of 200 years the depth of the pit will decrease with 10 metres, but still it will be 10 metres deeper than the surrounded area. At the beginning, compared to the other locations, the wavelength is large, but after 200 years the wavelength is the same as the other areas. The growth rate and the response time are significant smaller than the values of the sand wave fields. This means sand waves occur and grow slow, in other words on a large time scale. Compared to the original situation the orientation of the sand waves changes 15 ° South and will reduce to 2 ° South during the period of 200 years.

Table 5.5: The sand wave characteristics at the location 'Maximal depth in pit'

τ	x	y	θ	M_0	M_2	M_4	$\widetilde{\varphi}_{M4}$	h_0	Γ_r	L
years	[km]	[km]	[°]	[m/s]	[m/s]	[m/s]	[°]	[m]	[-]	[m]
Initial			90	0.072	0.744	0.053	321	24.0	0.05	376
10	1.3	0.5	101	0.049	0.482	0.039	323	43.1	0.00	858
50	1.8	0.4	100	0.056	0.500	0.039	320	41.1	0.00	777
100	2.8	0	96	0.066	0.523	0.038	320	39.0	0.00	696

Besides the model only calculates the sand wave dynamics with the given sediment size. If there is, or will be, silt present in the pit, no sand waves will occur Borsje et al. (2009). Therefore, an analysis is performed in order to find out what the influence is from the grain size of the sediment. The known parameters are velocity and depth, but the grain size is a rough estimation. With a grain size smaller than 0.13 mm or bigger than 0.96 mm no sand waves will occur, so it is plausible with the current circumstances sand waves will arise (0.13 mm $<$ grain size $<$ 0.96 mm).

`Conclusion`

The sand wave characteristics for the different position will not change significantly. Which means that the influence of the sandpits on the existing sand wave fields is not or a little present. So the present characterises and dynamics will hold on for years.

That the sand wave characteristics in the first years are more influenced, than after a longer time, is because the pit will flatten out and therefore the impact of the pit on the velocity is less present.

In the non-influenced area are no sand waves present, meanwhile the circumstances are suitable to form sand waves. There is the possibility that there is silt present in this area or that the circumstances differs because of the outlet of the river.

5.3. Practical application

The question that can be asked is what happens to the navigation channels to enter Rotterdam mainport. Therefore the navigation channels are implemented in the model. Because the dredging activities are not taken into account, the channel will migrate like a sandpit. Figure 5.13 shows the behaviour of the pits and the channel for the first fifty years. The morphological time is smaller than without the channel, because the interaction between the pit and the channel is then better visible.

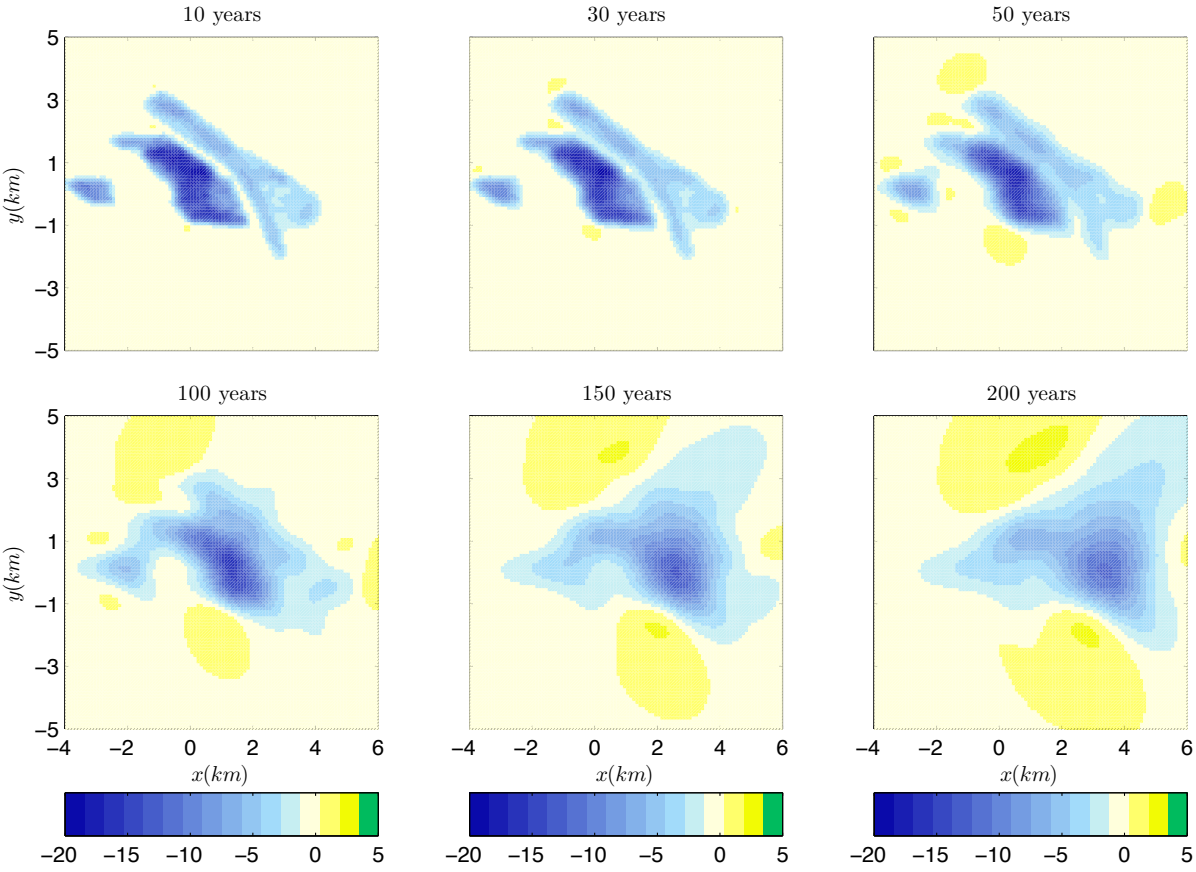

Figure 5.13: The morphodynamic behaviour of the pit with the navigation channel.

In Figure 5.13 it is visible that the ridge between the biggest sandpit and the navigation channels will vanish in time. Because the channels behave like a sandpit it will also migrate in the dominant flow direction, while in reality the positions are fixed caused by dredging activities. Because of the fixed positions the largest sandpit will reach the navigation channels sooner than the results show.

Figure 5.14 and 5.15 shows the transect of G and I, which are also taken in section 5.1. Here the difference is shown of the sandpit and the navigation over a period of 50 years. In the first period of thirty years the largest decrease of the ridge, between the channel and pit, will occur. In the second period, after thirty years, the ridge will decrease in a lower rate and finally it will vanish. It is also visible that the slopes will flatten out and the pit becomes shallower. However, the navigation channel becomes deeper because of the connection between the pit and channel, and it will start behaving like a pit. This means that the merged pit will migrate in the flow direction and the bottom will become flattened.

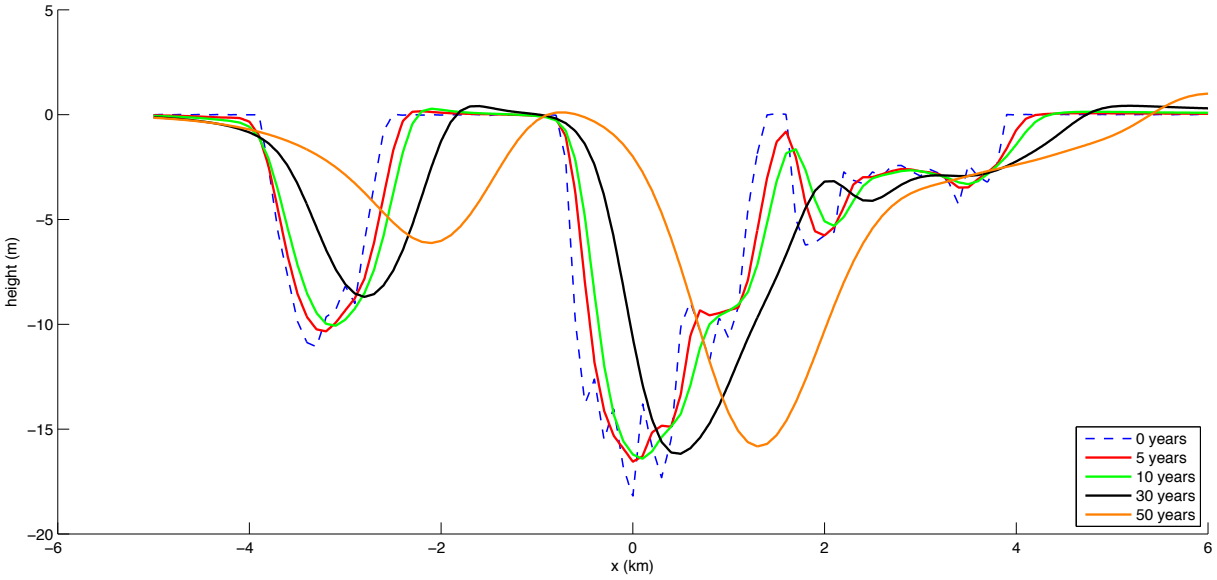

Figure 5.14: Transect G, including the navigation channel

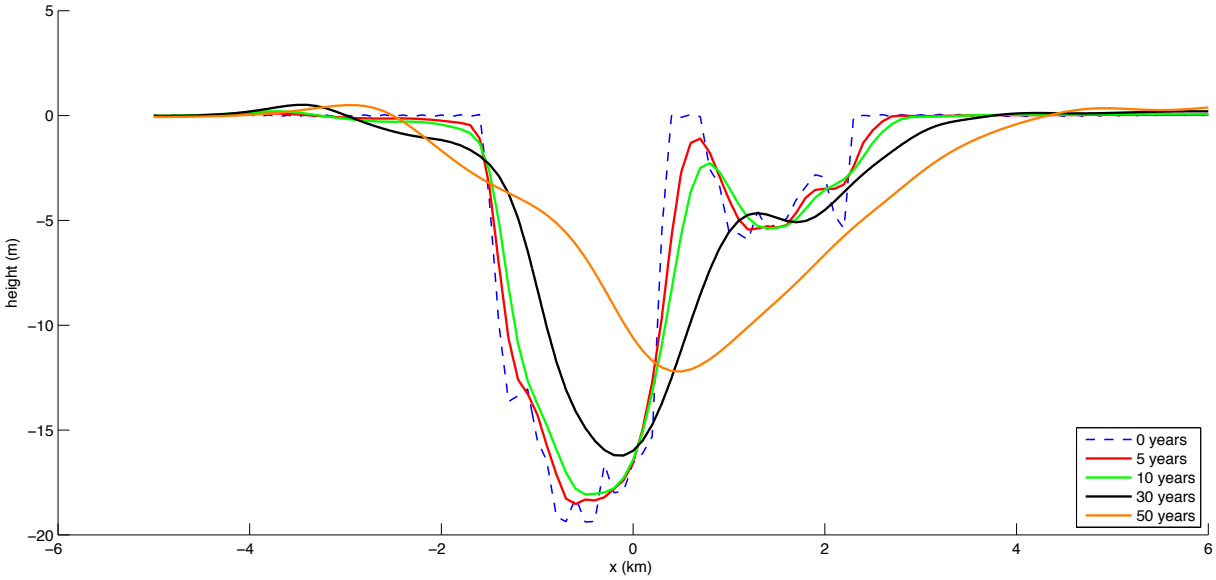

Figure 5.15: Transect I, including the navigation channel

The deepest point of the transect is followed to determine the migration in x-direction. This is done for both transects and illustrated in Figure 5.6, the migration rate is illustrated in Figure 5.17.

In the first couple of years the pits migrate faster, but after those years the migration is almost stable. The increasing of transect I is due to the merging of the pit with the channel. By this merging the deepest point is included with the channel and therefore the deepest point is harder to follow, which conclude in a larger migration rate, which is not comparable with the other years.

The ridge between the large pit and the navigation channel vanish in time. In transect G the edge will eroded for the first 30 years and will totally be connected with the large pit. In transect I the edge needs a smaller time to vanish, namely 10 years. Over the years the edge become smaller and the flow need less effort to reduce the edge, therefore the erosion of the edge becomes higher over the years.

It has to be noticed that the migration rate is higher in the first years when the navigation channel is implemented. However, the total migration over 200 years is the same as in the situation without the navigation channel.

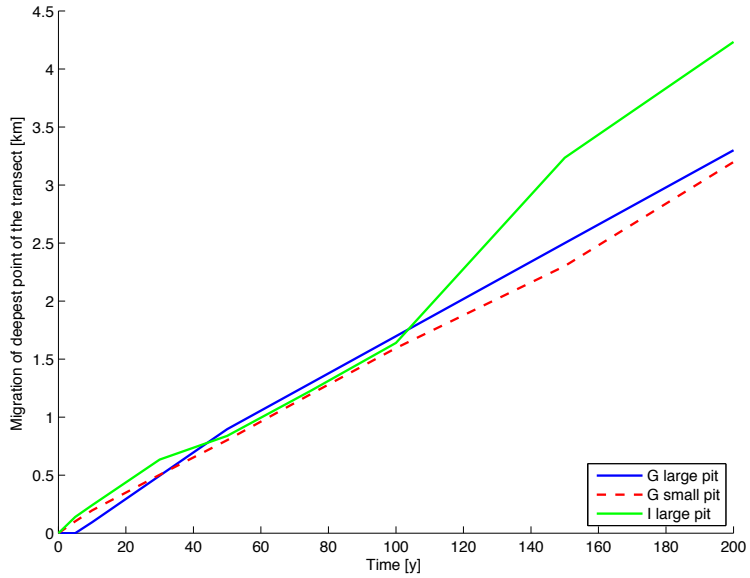

Figure 5.16: The total migration over the years [km] for Transect G and I

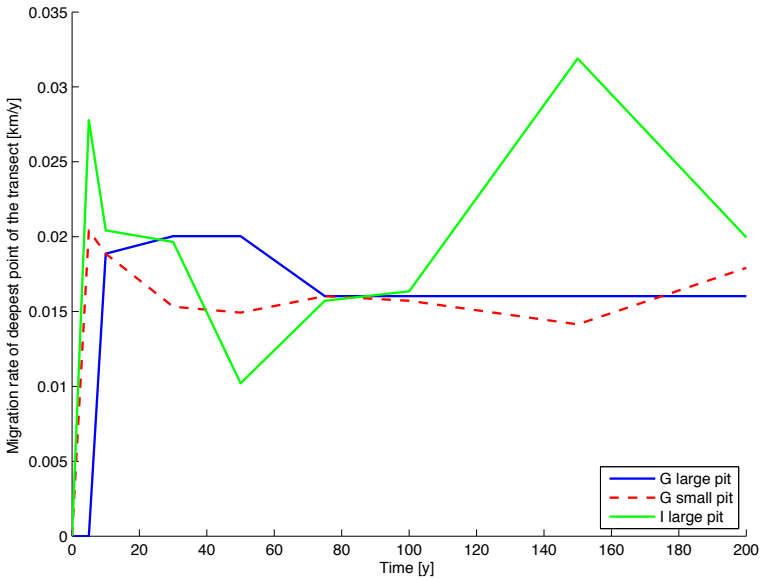

Figure 5.17: The migration rate over the years [m/y] for Transect G and I

5.4. Comparison with the results of Svašek

Klein and van den Boomgaard (2013) also did a research to the morphologic evolution of the sandpits. For the calculations two models were used: the wave model and the hydrodynamic model. The sea bed forms are used as input for both models. The output of these models are used as input for a sand transport model. Finally the output of the sand transport model is used as a new bed form and the process is repeated. The modelling is done with- and without the non-eroded layer between the pits. The simulation without the eroded layer can be compared with the results of the modelled sandpits and navigation channel (see section 5.3). Figure 5.18 gives a transect (Raai 3) which is comparable with the location of Transect G (see Figure 5.2 and 5.14).

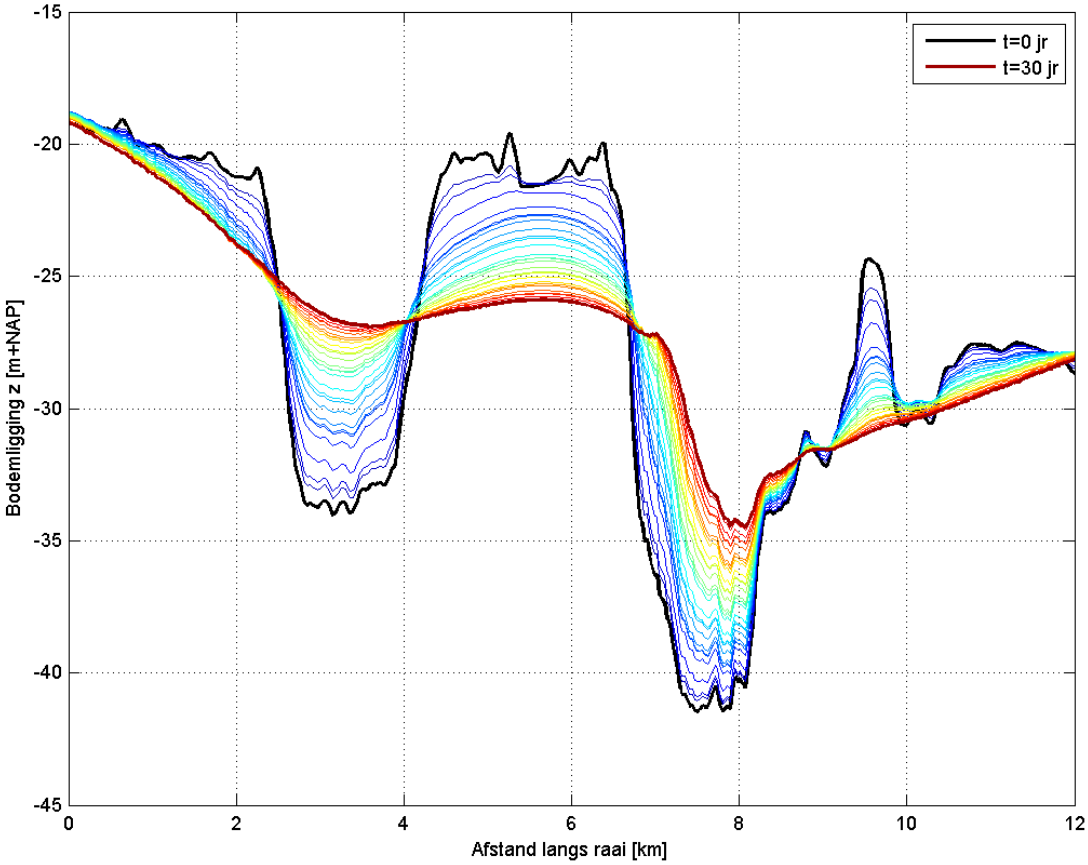

Figure 5.18: Transect Raai 3 on nearly the same location of Transect G (see Figure 5.14) (Klein and van den Boomgaard, 2013)

The largest difference between Transect G and Transect Raai 3 is that the pits are more shallow at Raai 3. Klein and van den Boomgaard (2013) modelled on a shorter morphological time scale, namely 30 years. So the long-term evolution of the pits can not be compared with each other. It seems that the sediment is deposit into the large pit and that the edge between the sandpits

will dashed out and also move into the larger pit. While this is not the case at our results, the edge between the pits will dashed out on that short-term. The absolute migration of the deepest point of the transect though, has the same magnitude. Over the first 30 years the large pit will migrate in the sandpit model with nearly 500 metres and Raai 3 about 600 metres. The migration rate is therefore comparable, this is only valid when looking to the deepest point of the sandpit. Looking with a broader view, the large pit on Raai 3 won't hardly migrate.

The large difference between the results may be due to the modelling method. Klein and van den Boomgaard (2013) combine a wave model with a hydronamic model, while the model of Roos et al. (2008) is only based on a hydrodynamic part. The model of Roos et al. (2008) does not take the suspended load into account, which may have a great influence on the sedimentation in the pits.

Chapter 6

Discussion

In this chapter the results are discussed based on the data analysis, the sandpit model, the sand wave model and finally the implication of the navigation channel.

Data analysis The data in and around the sand pit lacks in quantity and quality. Also there was not enough data collected with the single beam measurements to use the data for a good analysis of the sand waves/pit. In both instances there are many vertical displacements in the survey data of the sandpit surrounding. This has led to questioning the supplied datasets; the raw data is not available and the only available data are altered datasets which can not solely be trusted.

Useful data studies, which are used in the research, are gathered from the anchorage area, six kilometres away from the sandpit. Because of the minor influence of the sandpit the data analysis in the anchorage area is less valuable. From above description it can be concluded that de data analysis is possible, but that better datasets will lead to better results and more accurate conclusions.

The method that is used from (Van Dijk et al., 2008) shows for different transects in the same sand wave field, different migration rates. Therefore it is very difficult to determine the sand wave migration. It turns out that the migration rate is very dependable from the place and angle of the chosen transect, in other words the chosen transect is sensitive. It is to question if this method is the best option to determine the sand wave migration for this sand wave field.

Sandpit model The sandpit model is a linear model, it means that the hydrodynamics and sediment transport are linear in the ratio of pit depth and water depth. In reality this is not the case as nonlinear effects play a role. The linear model has a lot of practical benefits, for instance the complexity is manageable and the calculations are time-suficient. That absolute migration for the deepest point on Transect B and Transect Raai 3 are almost the same, this does not guarantee does not give guarantee that the long-term outcomes also will be the same (see section

5.4). The difference in the sedimentation of both models is that high, that the modelled sandpits of Klein and van den Boomgaard (2013) will behave different after the modelled 30 years. The large difference between the sedimentation in the pits may be due on the different model approaches. Where the model of Roos et al. (2008) not taken suspended load into account, in contrast to Klein and van den Boomgaard (2013). Besides, as noted above, the sandpit model is specifically designed for shallow pits, which means that the ratio between the pit- and water-depth has to be small. For this specific situation, this is not the case, the water depth (24 m) and the maximal pit depth (20 m) has almost a ratio that is equal to one. Also this may lead to inaccuracies in e.g. the migration rates.

The sandpit is modelled as a disturbance of an otherwise flat seabed. A morphodynamic model showing the presence of both stable and unstable modes. The same models are used to show that an unstable seabed gives rise to tidal sandbank formations (De Vriend, 1990; Hulscher et al., 1993). The instability is local at the sandpit, which causes a topographic waviness with a certain orientation and wavelength. According to (Roos et al., 2004) any pit will trigger this instability because any pit contains unstable modes.

What could be an issue is the slope of the seabed, see Figure 4.5. The smaller pit is located at a deeper position compared to the larger pit. This causes changes in the water depth, which results in changes in flow velocity. The model does not take the slope data into account. Therefore an adaptation is made in the calculations to even out the slope. The larger sandpit is simulated at the same height as the smaller pit, which will change the underlying relation of the two pits and probably the long-term effects will change.

The tidal velocity, which is used in the sandpit model, is based on the data of one season, namely Spring. In other words Spring will represent the whole year cycle. The tidal velocity consists of tidal components, which are all projected on the major axis of the M2-tide. This means that the ellipsoidal tides are transformed into a vector. With this transformation the tidal velocity loses a part of its strength and the rotation is eliminated.

It has to be noted that there is a non-erosive clay layer between the two pits (Klein and van den Boomgaard, 2013). In reality the migration from the smaller to the larger pit, simulated in this model, will probably not occur or this process takes longer.

Sand wave model The sand wave model has a simplified nature, uses a linear stability analysis and gives the results in sand wave occurrence or not. The model gives the possibility of performing a weakly non-linear stability analysis able to predict the equilibrium amplitude of the bottom forms. The linear stability analysis is unable to provide any information on the equilibrium amplitude attained by a growing perturbation for a long time. The model uses three variable inputs, namely the local depth, grain size and the M2-velocity. Therefore no other tide components are taken into account. This ensure that the model time is small and there can be made an approximation if sand waves will occur or not.

An important factor in the model calculation is the grain size of sand. In the natural formation sand is always divided in multiple grain sizes. The grain sizes found in the sandpit are grouped in 5 ranges. Because the model can only take one grain size in consideration, the average size of the range that covers the largest part (50%) of the measured grain sizes is used. Since the results are based on one grain size the results can be disputed.

Theoretically this could lead to the usage of a larger grain size than when the model could take whole ranges of grain sizes. Compared to the use of smaller grain sizes the larger grain sizes can cause less sand waves. In relation to the conclusion of the amount of sand waves, the results of the research could be sparse.

Because the sandpit becomes shallower, it is highly probable that sand, sediment and silt will deposit on the bottom of the sandpit. Due to the composition of silt the top layer of silt will stop the forming sand waves (Borsje et al., 2009). The results of the research of the forming of the sand waves are therefore not absolutely certain.

Navigation channel In the execution of the sand pit model the navigation channel is added as a factor. The model considers this as an extra sand pit with all of its consequences. In reality the navigation channel is not subjected to the morphological changes as much as in the sand pit. The reason is that the Rijkswaterstaat puts a lot of effort in the dredging and maintenance of the navigation channel. The most predictable possibility is that the sand pit will merge sooner with the navigation channel than predicted.

The exact consequences are hard to predict, because in all the measurements and model results it cannot be foreseen how the sand pit will behave in comparison to the navigation channel. It has to take into account, that in this model still the not eroded clay layer is not modelled. The consequence of this layer can still be only estimated. My best assumption is that the sandpits will merge at least later than it is calculated by the model and that the navigation channel is a serious factor to consider in future calculations.

Chapter 7

Conclusion

In this chapter the research questions are repeated and answered briefly. This thesis concerns of the evolution of the sand extracting pit and the surrounding sand wave fields. The research objective, is formulated as follows:

The understanding of the morphodynamic behaviour of the sandpit and the sand wave characteristics in and outside the sandpit.

The conclusion of this thesis is given by answering the research questions.

Which morphological behaviour in- and outside the sandpits are visible over 200 years according to the model from Roos et al. (2008)?
The morphological behaviour in- and outside the sandpits is the most active in the first 50 years. After 200 years the morphological effects are mostly drawn out, as far as we can see for now.

The most prominently morphological effect (according to the model from Roos et al. 2008) is the migration of the small pit towards the larger pit. At one point in the model the two pits will merge together in one large pit, see Chapter 4.

The migration of the two pits will follow the dominant flow direction, in this case towards the navigation channel. The model results show the pit will migrate thus far to the navigation channel that edge between the pit and navigation channel will dash out.

The morphological changes will cause the edges to flatten out, and eventually the pit become more shallow, which was expected upfront.

Are there sand waves arising into the pit?
The circumstances are sufficient enough in order to ensure that sand waves will arise. The velocity and depth are high enough to create sand waves, even with a grain size of 0.96 mm sand waves were still forming according to the model. So if only the modelled data is considered it is most likely sand waves will form in the pit.

When a broader view on the subject is taken into account, it will be probable that silt will form on the seabed in the pit. The formation of silt will stop the formation of sand waves completely. So the conclusion is that the formation of sand waves in the sand pit in reality will most likely not occur.

What is the influence from the sandpit on the surrounding sand wave fields and are these influences also visible in the data?
The influence from the sandpit on the surroundings is little to none. According to the modelled data the sand waves remain at the same lengths. The initial conditions are not subjected to change. The only visible difference in the output is a direction shift in the migration of 2 degrees. Taken into account that a simplified model is used, it would be very plausible that the migration shift is not noticeable in reality.

With the bathymetric data which is analysed in the anchorage area, some kilometres away from the pit, the influence of the sandpit was nearly visible. The calculated migration rate is very dependable of location and angle of the transect in the sand wave field. Therefore there is not a difference visible in the years what could be influenced by the sandpits. The bathymetric data confirms the conclusions of the modelled sand wave characteristics.

The conclusion is that the sandpit has no visible influence on the sand wave fields in the surroundings of the sandpit.

In summary, the sandpit will migrate with the dominant flow direction towards the navigation channel. The edges will flatten out and the pit becomes more shallower. This concludes in a larger 'sandpit' area. The surrounding sand wave fields, keep their characteristics and the magnitude will not change significantly, Which means that the sand wave fields are stable and the migration direction of the sand waves will not differ. Inside the pit the circumstances are right to form sand waves, only this occurrence can be put in doubt because it is assumable that silt covers the pit. With silt no sand waves will occur.

Chapter 8

Recommendations

Research is never ending, so also this one is not. In this chapter recommendations are given for further research, they are categorised per subject.

When looking to the available bathymetric data not all the data was of good quality or not in frequency that is needed for comparison. In 2015 a new survey will be performed by the Hydrographic Service. My recommendation is to compare the migration rate in the surrounding of the pit between the HY14105 and the survey of 2015. With this analyse it can be concluded if the modelled sand wave characteristics match with the actual characteristics. Especially the sand wave fields southwest of the sandpits are interesting. It may be better to use another method for determine the actual migration rate or at least analyse more transect to give a better view on the migration rate.

With the future survey of 2015 it will be visible what the behaviour of the pits is over three years. It would be interesting to compare the changes and behaviour with the modelled behaviour over 5 years. If the sand pits show more flattened edges, a migration of the deepest depths in the pit along transect G and not a lot of sedimentation. The modelled sandpits behaviour is an estimation which can be taken into account. If there is a lot of sedimentation in the pit, the modelled estimation of Klein and van den Boomgaard (2013) is more accurate.

The spatial range of the sandpit model is chosen for 25.6 kilometres and the influence of the pits reaches until the boundaries. Therefore it will be recommended to expand the spatial range in further research. The sandpit model does not take the slope, non-eroded clay layer between the pits and the sand wave patterns into account. The model would be more accurate when these factors are included in the calculation. A disadvantage is that this would mean that the model has to be adapted This is not the purpose of the model and this may would be too complex.

The difference between the visible results of Klein and van den Boomgaard (2013) and our results are large, I would recommend to identify the reasons of the differences, it is interesting to investigate the causes of that.

In this research the navigation channels are not taken into account, though not as permanent objects. In this study the navigation channels are implemented in a few analysis and act as sandpits. In reality those channels will stay in place and are kept on a certain depth by dredging activities. It is recommended to do this study again with a stable navigation channel. Besides it is recommended to keep monitoring the navigation channel to ensure the dredging activities are frequent enough. It is expected that the sand waves will not migrate faster into the navigation channel, but the effect of the sandpit migrating into the channel is uncertain with respect to the dredging activities.

The sand wave model is only used to determine if at a specific place sand waves will occur and if they do, what the characteristics of the waves are. The migration and growth rate in y-direction are disregarded. The reason why this is not done is because there are no changes of sand wave characteristics over the morphological timescale. There were also not a lot of differences between the initial situations with and without the sandpits. If there are other modelled situations, it is recommended to involve the migration and growth rate in y-direction to find out if the sand wave characteristics are dynamic over time.

The dimension of the sand extraction pits does not influence the sand wave fields. Which means that the size of the pits has small flow velocity influences on the seabed, but the influence on the water surface is much larger. When a sand extraction pit is close to a navigation channel the navigation will experience the changes in flow velocity in and around the pits. Also there is a possibility that the sandpits will migrate into the navigation channel, which can cause unsafe situations. Therefore it is recommended that the locations of future sand extraction pits are not in the close vicinity of navigation channels or busy waterways, which will also reduce the amount dredging activities.

This research is based on decreasing of the seabed, namely a sandpit. For the navigation this is less interesting, but shallow waters are very important for safe navigation. In the future it is interesting to research the dump areas, where the sea bed is increasing. How will the increasing sea bed behave over a certain time period? Is safe navigation still guaranteed?

Bibliography

AAPA (2004). World of port rankings. Technical report, American Association of Port Authorities.

Besio, G., Blondeaux, P., Brocchini, M., and Vittori, G. (2004). On the modeling of sand wave migration. *Journal of Geophysical Research*, 109(April).

Besio, G., Blondeaux, P., and Vittori, G. (2006). On the formation of sand waves and sand banks. *Journal of Fluid Mechanics*, 557:1.

Boers, M. (2005). Effects of a deep sand extraction pit. Technical report, Ministerie van Verkeer en Waterstaat.

Borsje, B. W., Hulscher, S. J. M. H., Herman, P. M. J., and De Vries, M. B. (2009). On the parameterization of biological influences on offshore sand wave dynamics. *Ocean dynamics*, 59(5):659–670.

Borsje, B. W., Roos, P. C., Kranenburg, W. M., and Hulscher, S. J. M. H. (2013). Modeling tidal sand wave formation in a numerical shallow water model: The role of turbulence formulation. *Continental shelf research*, 60:17 – 27.

Cherlet, J., Besio, G., Blondeaux, P., Van Lancker, V., Verfaillie, E., and Vittori, G. (2007). Modeling sand wave characteristics on the Belgian Continental Shelf and in the Calais-Dover Strait. *Journal of Geophysical Research*, 112(C6):C06002.

Choy, D. Y. (2015). Numerical modelling of the growth of offshore sand waves. Master thesis, TU Delft, National University of Signapore.

De Boer, W. P., Roos, P. C., Hulscher, S. J. M. H., and Stolk, A. (2011). Impact of mega-scale sand extraction on tidal dynamics in semi-enclosed basins: an idealized model study with application to the southern north sea. *Coastal engineering*, 58(8):678–689.

De Groot, P. J. (2005). Modelling the morphological behaviour of sandpits: Influence sediment transport formula and verification of a 1dh model. Master thesis, Civil Engineering and Management, University of Twente.

De Vriend, H. J. (1990). Morphological processes in shallow tidal seas. In Cheng, R. T., editor, *Residual Currents and Long-term Transport*, volume 38 of *Coastal and Estuarine Studies*, pages 276–301. Springer New York.

Dienst der Hydrografie (2013). *HP33, Waterstanden en stromen lang de Nederlandse kust en aangrenzend gebied*. De staat der Nederlanden, 2013 edition.

Dijkshoorn, C. and Stolk, A. (2009). Sand extraction maasvlakte 2 project: License environmental impact assessment and monitoring.

Dodd, N., Blondeaux, P., Calvete, D., de Swart, H. E., Falques, A., Hulscher, S. J. M. H., Rozynski, G., and Vittori, G. (2003). Understanding coastal morphodynamics using stability methods. *Journal of coastal research*, 19(4):849–865.

Dorst, L. L. (2009). *Estimating Sea Floor Dynamics in the Southern North Sea to Improve Bathymetric Survey Planning*. PhD thesis, University of Twente.

Havenbedrijf Rotterdam (2009). Van plan tot uitvoering.

Hoogewoning, H. E. and Boers, M. (2005). Physical effects of sea sand extraction. Technical report, The Netherlands Ministry of Transport, Public Works and Water Management.

Hoogewoning, S. E. and Boers, M. (2001). Physical Effects of Sea Sand Extraction. Technical report, The Netherlands Ministry of Transport.

Hulscher, S. J. M. H. (1996). Tidal-induced large-scale regular bed form patterns in a three-dimensional shallow water model. *Journal of Geophysical Research*, 101:20,727–20,744.

Hulscher, S. J. M. H., de Swart, H. E., and De Vriend, H. J. (1993). The generation of offshore tidal sand banks and sand waves. *Continental Self Research*, 13:1183–1204.

Huthnance, J. H. (1982). On one mechanism forming linear sand banks. *Estuarine, Coastal and Shelf Science*, 14(1):79 – 99.

JOC (2012). The joc top 50 world container ports.

Johnson, M. A., Stride, A. H., Belderson, R. H., and Kenyon, N. H. (2009). *Predicted Sand-Wave Formation and Decay on a Large Offshore Tidal-Current Sand-Sheet*, pages 247–256. Blackwell Publishing Ltd.

Klein, M. D. (1999). Large-scale sandpits- hydrodynamic and morphological modelling of large-scale sandpits.

Klein, M. D. and van den Boomgaard, M. (2013). Evaluatie van zandwinputten MV2. Technical Report september, Svašek Hydraulics, Rotterdam.

Knaapen, M. A. F. and Hulscher, S. J. M. H. (2002). Regeneration of sand waves after dredging. *Coastal Engineering*, 46:277–289.

Langhorne, D. N. (1981). An evaluation of bagnold's dimension- less coefficient of proportionality using measurements of sand wave movements. *Marine Geology*, 43(5):49–64.

Morelissen, R., Hulscher, S. J. M. H., Knaapen, M. A. F., Németh, A. A., and Bijker, R. (2003). Mathematical modelling of sand wave migration and interaction with pipelines. *Coastal Engineering*, 48:197–209.

Nemeth, A. A., Hulscher, S. J. M. H., and De Vriend, H. J. (2002). Modelling sand wave migration in shallow shelf seas. *Continental Shelf Research*, 22(18-19):2795–2806.

Pawlowicz, R., Beardsley, B., and Lentz, S. (2002). Harmonic analysis including error estimates in matlab using t_tide. *Computers and Geosciences*, 28:929–937.

Port of Rotterdam (2014). Zandwinning op zee.

Roos, P. C., Hulscher, S. J. M. H., and De Vriend, H. J. (2008). Modelling the morphodynamic impact of offshore sandpit geometries. *Coastal Engineering*, 55:704–715.

Roos, P. C., Hulscher, S. J. M. H., Knaapen, M. A. F., and van Damme, R. M. J. (2004). The cross-sectional shape of tidal sandbanks: Modelling and observations. *Journal of Geophysical Research*, 109.

Schipper, S. (2014). Bachelor Eindopdracht Morfodynamische verwachtingen voor het zandgolfveld ten westen van de Maasvlakte 2.

Svašek (2001a). Putmor field measurements at a temporary sand pit, part 1: Processing and validation. Technical report, Svašek b.v.

Svašek (2001b). Putmor field measurements at a temporary sand pit, part 2: Data analysis. Technical report, Svašek b.v.

Svašek (2001c). Putmor field measurements at a temporary sand pit, part 3: Final report. Technical report, Svašek b.v.

The Netherlands Hydrographic Service (2013). Hp33d, nltides. Dvd.

The Netherlands Hydrographic Service (2015). Hp33d, nltides. Dvd.

Thorn, M. (1987). Coastal and estuarine sediment dynamics by k.r. dyer. wiley, chichester, 1986. no. of pages: 358. *Geological Journal*, 22(2):169–169.

Tobias, F. C. (1988). *Morphology of Sandwaves in Relation to Current, Sediment and Wave Data Along the Eurogeul, North Sea: Interim Report*. Rapport GEOPRO. Geografisch Instituut, Rijksuniversiteit Utrecht.

Tonnon, P. K., Van Rijn, L. C., and Walstra, D. J. R. (2007). The morphodynamic modelling of tidal sand waves on the shoreface. *Coastal Engineering*, 54:279–296.

Van der Veen, H. H., Hulscher, S. J. M. H., and Knaapen, M. A. F. (2006). Grain size dependency in the occurrence of sand waves. *Ocean Dynamics*, (56):228–234.

Van Dijk, T. A. G. P., Kleinhans, M. G., and Egberts, P. J. P. (2008). Separating bathymetric data representing multiscale rhythmic bed forms: A geostatistical and spectral method compared. *Journal Geophysical Research*, 113.

Van Rijn, L. C. and Walstra, D. J. R. (2004). Analysis and modelling of sand mining pits. Technical report, WL — Delft Hydraulics.

Van Rijn, L. C. and Walstra, D. R. (2002). Morphology of Pits , Channels and Trenches. Technical Report January, WL— Delft Hydraulics, Delft.

Van Tongeren, O. (2013). Sediment zandwinning effectmeting 2006-2013. Technical report, Port of Rotterdam, Dataneco.

Appendix A

Bathymetric data analysis

In this appendix tables of the bathymetric data can be found. Table A.1 and Table A.2 give the sand wave characteristics of Transect A and B respectively. The sand wave characteristics consist of the total wave length and the ratio between the Lee and Toss side of the sand wave. These terms are illustrated in 2.2. Based on these characteristics the migration rate is determined with a linear regression method (see section 3.3.2). The migration rate for each sand wave of each transect is shown in Table A.3 and Table A.4. The migration rate of the transect are also shown in Figure 3.10 and 3.11.

A.1. Calculated sand wave characteristics

Table A.1: The sand wave length in metres and the ratio between the stoss length and lee length of the sand waves from Transect A. Data is gathered from the transect which is shown in Figure 3.4.

Sandwave	**Length**					**Ratio Lstoss/ Llee**				
	2006	2008	2011	2013	2014	2006	2008	2011	2013	2014
1	145	146	146	149	148	2.3	2.5	2.3	2.4	2.3
2	96	93	87	86	86	0.8	0.7	0.8	0.8	0.8
3	135	136	137	138	137	2.0	2.1	2.2	2.2	2.1
4	123	121	123	122	122	1.8	1.8	1.8	1.9	1.9
5	137	139	138	140	141	2.0	2.0	2.0	2.0	2.0
6	136	143	134	133	135	1.7	1.5	1.8	1.9	1.8
7	103	96	102	103	101	1.5	1.3	1.5	1.6	1.5
8	85	86	81	82	79	0.9	0.8	0.8	0.8	0.8
8	124	125	126	126	126	2.0	2.0	1.9	1.9	1.9
10	114	114	114	112	110	1.8	1.8	1.8	1.9	2.0

Table A.2: The sand wave length in metres and the ratio between the stoss length and lee length of the sand waves from Transect B. Data is gathered from the transect which is shown in Figure 3.4.

Sandwave	**Length**					**Ratio Lstoss/ Llee**				
	2006	2008	2011	2013	2014	2006	2008	2011	2013	2014
A	98	103	105	104	106	1.9	2.0	2.0	2.1	2.1
B	108	107	105	103	104	1.6	1.5	1.7	1.8	1.7
C	143	141	142	143	142	2.5	2.4	2.6	2.8	2.8
D	99	98	98	98	97	1.7	1.6	1.7	1.8	1.8
E	132	134	138	140	141	2.2	2.5	2.8	2.9	3.0
F	79	76	74	69	68	0.7	0.7	0.7	0.8	0.8
G	84	86	88	91	92	1.1	1.1	1.2	1.3	1.4
H	94	92	91	92	91	1.4	1.4	1.4	1.5	1.4
I	107	110	106	105	106	1.8	1.8	1.8	1.9	1.8
J	122	121	121	121	120	1.6	1.6	1.8	1.8	1.8
K	136	132	134	136	134	2.2	2.3	2.2	2.4	2.4
L	95	98	98	98	100	1.4	1.6	1.8	1.8	1.8
M	81	82	83	82	80	1.1	1.1	0.8	0.8	0.9

A.2. Calculated sand wave migration rates

Table A.3: Migration of the sand waves from Transect A in metres a year from the anchorage area, overall, before and after the realisation of the extracted sandpit.

Sand wave number	Overall	Before	After
1.	5.8	6.9	5.8
2.	5.5	4.0	5.1
3.	5.0	5.3	4.7
4.	5.1	4.3	4.7
5.	5.0	4.3	5.1
6.	5.3	3.9	5.8
7.	4.9	3.9	3.8
8.	4.2	3.9	5.3
9.	4.0	4.6	3.4
10.	4.3	4.7	2.6

Table A.4: Migration of the sand waves from Transect B in metres a year from the anchorage area, overall, before and after the realisation of the extracted sandpit.

Sand wave character	Overall	Before	After
A.	5.0	5.4	4.9
B.	5.0	4.3	5.5
C.	4.8	3.2	5.5
D.	4.4	2.2	5.3
E.	5.8	5.5	6.4
F.	4.7	3.6	5.1
G.	5.0	2.6	6.4
H.	4.5	2.9	4.9
I.	4.2	3.3	5.1
J.	4.3	4.0	6.4
K.	4.2	2.9	4.9
L.	5.0	4.4	4.7
M.	3.6	3.6	4.7

Appendix B

Calculation method on tides

When Maasvlakte 2 was realised a lot of new calculations had to be made. Because the Maasvlakte 2 is such a large area, a lot of conditions changed, including the flow. Figure B.1 illustrates the situation for two different years, before and after the realisation. It should be noticed that the flow- velocity and -direction are changed around the Maasvlakte 2.

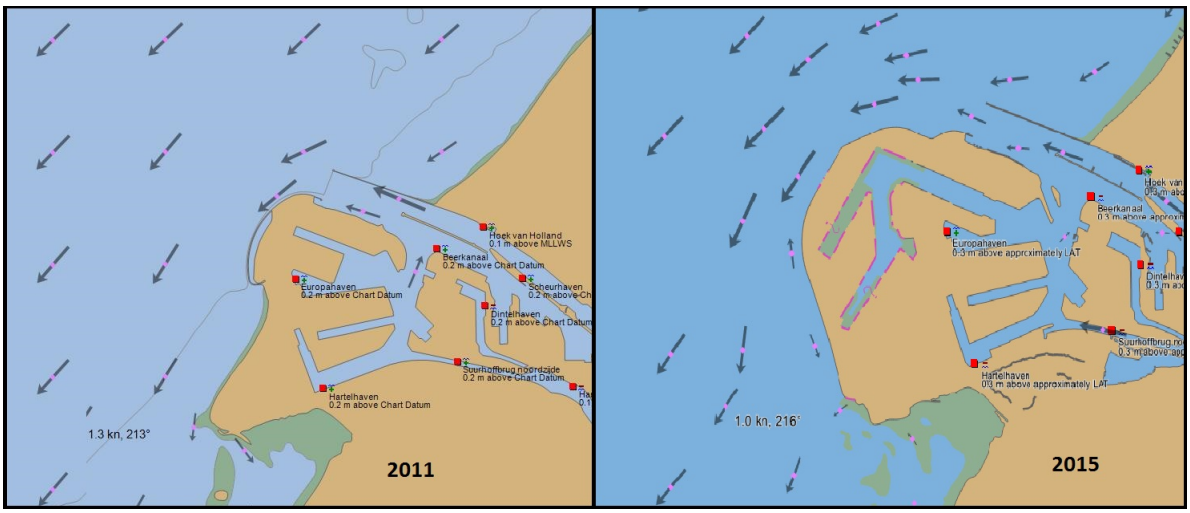

Figure B.1: Screenshots of NL tides where the difference in flow direction is visible for 2011 and 2015 (The Netherlands Hydrographic Service, 2015)

The program NL Tides (The Netherlands Hydrographic Service, 2013) is used to gather the velocities and directions of the flow, with these velocities the tidal flow can be calculated. A total spring neap cycle is gathered for the four seasons of the year to give an overview of the different tides. A spring neap cycle is the period between full- and new moon, in this cycle all the tide periods are included and can be calculated. The velocity vectors can be divided in an east- and north component. The program t_tide which is made by Pawlowicz et al. (2002) calculates the different tidal components with their amplitude and phase. This is done by a Fourier-analysis, which divides a signal in different smaller signals, where every signal has its own period. The t_tide model divides the total signal of the x- and y- component to the tidal consistent. The results for the residual flow, M2- and M4 tide are shown in Table B.1 and ellipses and vector are illustrated in Figure B.2.

Table B.1: Values for the x- and y- components for each season, output from t_tide.

			Autumn	**Spring**	**Summer**	**Winter**
			5 to 19-10-2013	10 to 25-4-2013	8 to 22-7-2013	11 to 27-1-2013
M0	[m/s]	u	-0.0132	-0.0127	-0.0134	-0.0138
		v	0.0509	0.0504	0.0515	0.0499
M2	[m/s]	u	0.4882	0.4894	0.4922	0.4850
		v	0.5638	0.5656	0.5683	0.5598
	[°]	u	97.25	124.82	130.79	143.92
		v	104.87	132.41	138.38	151.54
M4	[m/s]	u	0.0633	0.0607	0.0583	0.0589
		v	0.0376	0.0370	0.0374	0.0352
	[°]	u	65.99	122.06	134.25	159.08
		v	138.01	199.63	213.84	213.22

The residual tide is a constant velocity and caused by the difference between low- and high- tide. The largest tidal constituents is the M2 tide, this tide is called 'principal lunar semi-diurnal' and the total period of this constituent is the total spring neap cycle. Next to the M2 also the M4 tidal component can be included in the sandpit model which has the total period of half of the spring neap cycle. The residual flow is not calculated with t_tide, but calculated by the average of all the x- and y- components.

Because of the small differences in the values of the seasons, the season of spring is chosen to be the representative values for the rest of the calculations. All the tidal components have to projected onto the major axes of the dominant tide (M2). This is illustrated in Figure B.3, it should be noticed that by this approximation the flow velocity will slightly decrease and have another direction.

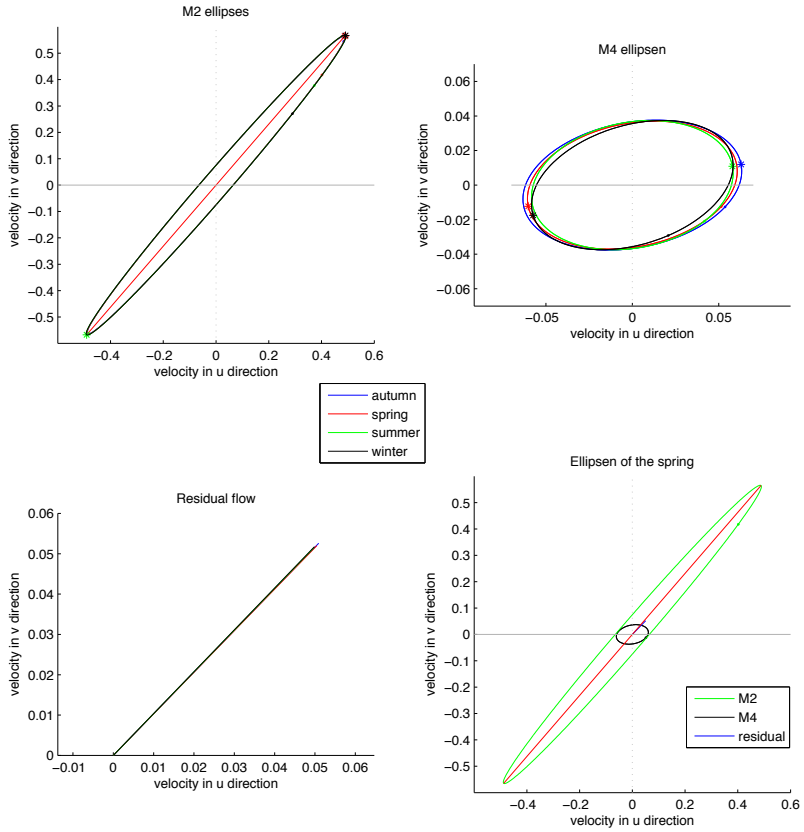

Figure B.2: Flow in different seasons

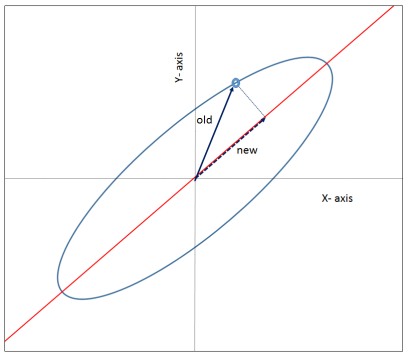

Figure B.3: Flow in different seasons

B.1. Velocity output of the sandpit model

The model calculates the influence of the extracted sandpit compared to the implementation of the sandpit. In other words:

$$J_{total}(t) = \hat{J}(t) + (u(x,y,t), v(x,y,t)) \tag{B.1}$$

Were $\hat{J}(t)$ is the initial situation before the pit is implemented. $u(t)$ is the velocity influenced by the pit in x direction and $v(t)$ is the velocity influenced by the pit in y direction. Together they give the total velocity, inclusive the influence of the modelled sandpit. Now the calculation can be made for the u-direction, this is the same for the v-direction.

$$u = \sum_{p=-p}^{p} \widetilde{U}_p(x,y) \exp(ip\hat{t})$$

$$u = \widetilde{U}_{-2}(x,y)\exp(-i2t) + \widetilde{U}_{+2}(x,y)\exp(+i2t)\widetilde{U}_{-1}(x,y)\exp(-it) + \widetilde{U}_{+1}(x,y)\exp(+it) + u_0$$

$$\begin{aligned} u = {} & (\widetilde{U}_{-2re} + i\widetilde{U}_{-2im})(\cos 2t - i\sin 2t) + (\widetilde{U}_{+2re} + i\widetilde{U}_{+2im})(\cos 2t + i\sin 2t) + \\ & (\widetilde{U}_{-1re} + i\widetilde{U}_{-1im})(\cos t - i\sin t) + (\widetilde{U}_{+1re} + i\widetilde{U}_{+1im})(\cos t + i\sin t) + u_0 \end{aligned}$$

$$u = 2U_{+2re}\cos 2t - 2U_{+2re}\sin 2t + 2U_{+1re}\cos t - 2U_{+1im}\sin t + u_0 \tag{B.2}$$

B.2. Transform the velocity output of the sandpit model to input for the sand wave model

As already mentioned in 4.2.1 the sandpit model gives an output in real- and imationair- tidal velocities. Those velocities has to be transformed back into a tidal signal, so they can be used as input for the sand wave model. How this transformation is done is explained beneath. The input is based on only the amplitude of the M2 tidal velocity, this means the output of the sandpit model has to be transformed back to Equation 4.5. The output of the sandpit model is illustrated with the formulas of Equation B.2. The following transition is needed to eliminated the components and arrive via Equation 4.6 at Equation 4.5.

$$\begin{aligned} M_{2total} &= M_2 \cos\hat{t} + 2u_{re}\cos\hat{t} - 2u_{im}\sin\hat{t} \\ M_{2total} &= \sqrt{(M_2 + 2u_{re})^2 + 2u_{im}^2} * \cos(\hat{t} - \tan^{-1}((M_2 + 2u_{re}), -u_{im})) \end{aligned} \tag{B.3}$$

$$\begin{aligned} M_{4total} &= M_4 \cos(2\hat{t} - \hat{\varphi}_{M4}) + 2u_{4re}\cos(2\hat{t}) - 2u_{4im}\sin(2\hat{t}) \\ M_{4total} &= \sqrt{(M_4\cos\hat{\varphi}_{M4} + 2u_{4re})^2 + (M_4\sin\hat{\varphi}_{M4} - 2u_{im})^2} * \\ &\cos(2\hat{t} - \tan^{-1}((M_4\cos\hat{\varphi}_{M4} + 2u_{4re}), (M_4\sin\hat{\varphi}_{M4} - 2u_{im})) \end{aligned} \tag{B.4}$$

Appendix C

Results at the different positions

The following results corresponds with the results which are described in Section 5.2.

`Sand wave field 1`

τ	θ	M_0	M_2	M_4	$\widetilde{\varphi}_{M4}$	h_0	Γ_r	**L**	T_r^*
years	[°]	[m/s]	[m/s]	[m/s]	[°]	[m]	[-]	[m]	[years]
0	92	0.062	0.749	0.060	318	24.0	0.05	377	7
10	92	0.064	0.758	0.060	318	24.0	0.05	375	7
30	92	0.067	0.767	0.061	321	24.0	0.06	379	7
50	92	0.067	0.766	0.060	324	24.0	0.06	379	7
75	91	0.068	0.763	0.060	324	24.0	0.06	376	7
100	91	0.069	0.761	0.059	324	24.0	0.05	375	7
125	91	0.069	0.759	0.059	324	24.0	0.05	380	7
150	91	0.070	0.757	0.058	324	24.0	0.05	379	7
200	91	0.071	0.754	0.057	324	24.0	0.05	378	7

`Sand wave field 2`

τ	θ	M_0	M_2	M_4	$\widetilde{\varphi}_{M4}$	h_0	Γ_r	**L**	T_r^*
years	[°]	[m/s]	[m/s]	[m/s]	[°]	[m]	[-]	[m]	[years]
0	95	0.069	0.720	0.053	321	24.0	0.04	372	9
10	95	0.070	0.725	0.053	321	23.8	0.04	369	8
30	94	0.071	0.739	0.054	321	23.6	0.05	372	8
50	94	0.072	0.743	0.054	321	23.7	0.05	373	8
75	94	0.072	0.747	0.055	321	23.8	0.05	374	7
100	93	0.073	0.753	0.055	321	23.9	0.05	371	7
125	93	0.074	0.755	0.055	321	24.0	0.05	372	7
150	93	0.074	0.753	0.055	321	24.0	0.05	377	7
200	92	0.075	0.750	0.054	321	24.0	0.05	374	7

`Anchor area`

τ	θ	M_0	M_2	M_4	$\widetilde{\varphi}_{M4}$	h_0	Γ_r	**L**	T_r^*
years	[°]	[m/s]	[m/s]	[m/s]	[°]	[m]	[-]	[m]	[years]
0	90	0.072	0.743	0.053	321	24.0	0.05	376	8
10	90	0.072	0.743	0.053	321	23.8	0.05	376	8
30	90	0.072	0.743	0.053	321	23.7	0.05	376	8
50	90	0.072	0.743	0.053	321	23.7	0.05	376	8
75	90	0.072	0.744	0.053	321	23.6	0.05	376	8
100	90	0.072	0.744	0.053	321	23.5	0.05	376	8
125	90	0.072	0.744	0.053	321	23.5	0.05	376	8
150	90	0.072	0.744	0.054	321	23.5	0.05	376	8
200	90	0.072	0.744	0.054	321	23.7	0.05	376	8

Non-influenced area

τ	θ	M_0	M_2	M_4	$\widetilde{\varphi}_{M4}$	h_0	Γ_r	**L**	T_r^*
years	[°]	[m/s]	[m/s]	[m/s]	[°]	[m]	[-]	[m]	[years]
0	90	0.071	0.742	0.054	321	24.0	0.05	376	8
10	89	0.071	0.742	0.054	321	24.0	0.05	376	8
30	89	0.071	0.741	0.054	321	24.1	0.05	375	8
50	89	0.070	0.739	0.054	321	24.1	0.05	374	8
75	89	0.069	0.736	0.054	321	24.2	0.05	373	8
100	89	0.068	0.732	0.054	321	24.3	0.05	372	8
125	89	0.066	0.727	0.053	321	24.4	0.05	376	9
150	89	0.064	0.722	0.053	321	24.5	0.04	374	9
200	90	0.062	0.719	0.053	321	24.3	0.04	370	9

Maximal depth in pit

τ	**x**	**y**	θ	M_0	M_2	M_4	$\widetilde{\varphi}_{M4}$	h_0	Γ_r	**L**	T_r^*
years	[km]	[km]	[°]	[m/s]	[m/s]	[m/s]	[°]	[m]	[-]	[m]	[years]
0	0.2	1.1	104	0.0571	0.5488	0.046	323	45.0	6.4E-03	738	211
10	1.3	0.5	101	0.0485	0.4819	0.0394	323	43.1	2.5E-03	858	502
30	1.5	0.5	101	0.0521	0.4917	0.0396	323	42.2	2.9E-03	815	402
50	1.8	0.4	100	0.0562	0.5	0.0391	320	41.1	3.4E-03	777	334
75	2.3	0.2	98	0.0612	0.5088	0.0383	320	40.0	3.9E-03	738	273
100	2.8	0	96	0.0661	0.5228	0.0383	320	39.0	4.7E-03	696	213
125	3.2	-0.1	95	0.0704	0.5391	0.0389	323	38.3	5.9E-03	656	164
150	3.6	-0.1	94	0.074	0.555	0.0398	323	37.4	7.2E-03	622	128
200	4.3	-0.1	92	0.0809	0.5877	0.0412	323	35.6	2.1E-02	429	40